Combined Heat and Power Units and Network Expansion Planning considering Distributed Energy Resources and Demand Response Programs

Saeed Qaeini[1], Mehrdad Setayesh Nazar[1], Farid Varasteh[1], Miadreza Shafie-khah[2], João P. S. Catalão[3*]

[1] *Shahid Beheshti University, Tehran, Iran*

[2] *School of Technology and Innovations, University of Vaasa, 65200 Vaasa, Finland*

[3] *Faculty of Engineering of the University of Porto and INESC TEC, Porto 4200-465, Portugal*

[*] *corresponding author: catalao@fe.up.pt*

Abstract

This paper addresses a hierarchical framework for the energy resources and network expansion planning of an Energy Distribution Company (EDC) that supplies its downward Active Industrial MicroGrids (AIMGs) with hot water and/or steam and electricity through its district heating and electric grid, respectively. The main contribution of this paper is that the proposed model considers AIMGs' electricity transactions with each other and/or other customers through the EDC's electric main grid and investigates the impacts of these transactions on the expansion planning problem. The solution methodology is another contribution of this paper that tries to trade-off between accuracy and computational burden. The proposed framework uses a three-stage iterative heuristic optimization algorithm that considers different uncertainties of the planning and operational parameters. At the first stage, the algorithm determines the characteristics of energy system facilities for different stochastic parameter scenarios. At the second stage, the feasibility and optimality of AIMGs' electric transactions are evaluated and the optimal scheduling energy resources in normal states are determined. Finally, at the third stage, different demand response alternatives, load shedding and the AIMGs' electric transaction interruptions for contingent conditions are decided. The proposed method is applied to 9-bus, 33-bus and 123-bus IEEE test systems. Further, a full search algorithm is used to evaluate the quality of solutions of the proposed algorithm. The introduced algorithm reduced the total costs for the 9-bus, 33-bus and 123-bus system about 18.645%, 9.658%, and 4.849% with respect to the costs of custom expansion planning exercises, respectively.

Keywords: Expansion planning; District heating; Distributed energy resources; Demand response programs, Electricity transaction.

Nomenclature

Abbreviation

AC	Alternative Current.
AIMG	Active Industrial Micro Grid.

CDF	Composite Damage Function.
CHP	Combined Heating and Power.
CO_2	Carbon dioxide.
DC	Direct Current.
DER	Distributed Energy Resource.
DCNEP	Distributed Cogeneration and Networks Expansion Planning.
DHN	District Heating Network.
DLC	Direct Load Control.
DRP	Demand Response Program.
EDC	Energy Distribution Company.
ESS	Electrical Storage System.
GA	Genetic Algorithm.
IAGA	Integrated Adaptive Genetic Algorithm.
HL	Heating Load.
IMG	Industrial Micro Grid.
MG	MicroGrid.
MILP	Mix Integer Linear Programming.
MINLP	Mixed Integer Non-Linear Programming.
MUs	Monetary Units.
MMUs	Million MUs.
MWRI	Modified Weighted Reliability Index.
PVA	Solar Photovoltaic Array.
PU	Per-unit.
QLDC	Quarterly Load Duration Curve.
SW	Switching device.
SWT	Small Wind Turbine.
TES	Thermal Energy Storage.

Index Sets

α	Electric system contingency index.
t	Time index.

Parameters and variables

S^{PVA}	Area of photovoltaic array (m^2).
$Boiler\_Site$	Boiler site.
BC	Boiler capacity selection alternatives.
TB_{PT}	Benefit of AIMGs electricity transactions (MUs).

TC_{CHP}	Investment, operational, emission and maintenance costs of CHP unit (MUs).
TC_{Feeder}	Investment costs of electric feeder (MUs).
TC_{Pipe_DHN}	Investment costs of district heating system pipe (MUs).
TC_{PVA}	Aggregated investment and maintenance costs of photovoltaic array (MUs).
TC_{SW}	Aggregated investment and maintenance costs of switching device (MUs).
TC_{SWT}	Aggregated investment and maintenance costs of small wind turbine (MUs).
TC_{ESS}	Aggregated investment, operational and maintenance costs of electricity storage (MUs).
TC_{TES}	Aggregated investment, operational and maintenance costs of thermal storage (MUs).
TC_{Boiler}	Aggregated investment, operational, emission and maintenance costs of boiler (MUs).
$TC_{Purchase}$	Cost of electricity purchased from upward utility (MUs).
TC_{DRP}	Cost of demand response program (MUs).
TC_{Invest}	Investment cost (MUs).
TC_{Op}	Operational cost (MUs/MWh).
TC_{M}	Maintenance cost (MUs/MWh).
TC_{EM}	Emission cost (MUs/kg).
Cap^{ESS}	Capacity of electricity storage (kW).
Cap^{TES}	Capacity of thermal storage (kW).
TC_{Inv}^{PVA}	Investment cost of photovoltaic array (MUs/MW.m^2).
TC_{Inv}^{TES}	Investment cost of thermal storage (MUs/MWh).
TC_{Inv}^{ESS}	Investment cost of electricity storage (MUs/MWh).
$TC_{Capacity}^{Feeder}$	Capacity dependent cost of electric feeder (MUs/m.kW).
Cap^{Feeder}	Capacity of electric feeder (kW).
TC_{leng}^{Feeder}	Length dependent cost of electric feeder (MUs/m).
$TC_{Capacity}^{DH}$	Capacity dependent cost of district heating system pipe (MUs/m.MW).
Cap^{DH}	Capacity of district heating system pipe (MW).
CHP_Site	CHP installation alternative site.
$CHPC$	CHP capacity selection alternatives.
CDF	Composite damage function (MU/MWh).
$DRPA$	DRP alternatives.
DH_Site	District heating site.
$ESSC$	Electricity storage capacity selection alternatives.
ESS_Site	Electricity storage installation alternative site.
EM_{CO_2}	CO_2 emission (ton/yr).
EM_{SO_2}	SO_2 emission (kg/yr).

EM_{NO_X}	NO_X emission (kg/yr).
EMC_{CO_2}	CO_2 emission penalty cost (MUs/ton.yr).
EMC_{SO_2}	SO_2 emission penalty cost (MUs/kg.yr).
EMC_{NO_X}	NOX emission penalty cost (MUs/kg.yr).
HL_Site	Heating load site.
I	Solar irradiation (kW/m).
L	Distance between energy carrier generation site and load site (m).
L_P	Weighted decibels (dBA).
$Load\_Site$	Electrical load site.
$NOIS$	Total number of AIMG's energy consumption scenarios and the EDC's intermittent electricity generation.
$NOSS$	Total number of electricity transactions of AIMGs scenarios.
$NCSS$	Total number of contingency scenarios.
$Ncont$	Number of EDC contingencies.
$Nyear$	Number of planning year.
$Nzone$	Number of EDC zones.
P_{shed}	Shed electrical energy (kW).
P^{BT}	AIMG electricity transaction (kW).
P^{EDC}	Electric power of EDC (kW).
P^{DRP}	Active power of DRP (kW).
P^{Load}	Electric power of electrical load (kW).
P^{PVA}	Electric power generated by photovoltaic array (kW).
P^{ESS}	Electric power delivered by electricity storage (kW).
$P^{Load}_{Critical}$	Critical electrical load (kW).
$P^{Load}_{Controllable}$	Controllable electrical load (kW).
P^{SWT}	Electric power generated by SWT.
ΔP^{DLC}	Electric power withdrawal changed for DLC program (kW).
PVA_Site	Photovoltaic array site.
Q'^{DRP}	Reactive power of DRP (kVAR).
Q^{Load}	Thermal load (kW_{th}).
Q^{CHP}	CHP thermal power output (kW_{th}).
Q^{Loss}	Loss of thermal power (kW_{th}).
Q^{Flow}	Thermal power flow in district heating system pipe (kW_{th}).
Q^{TES}	Thermal power of TES (kW_{th}).
R^{DHN}	Radius of district heating pipe (m).
R^{SWT}	Small wind turbine blade radius (m).

SWT_Site	Small wind turbine site.
TC_{leng}^{DH}	Length dependent cost of district heating system pipe (MUs/m).
TC_{IC}	Total interruption cost.
$TESC$	Thermal storage capacity selection alternatives.
TES_Site	Thermal storage installation alternative site.
A^{TES}	Binary variable of heating storage discharge; equals 1 if heating storage is discharged.
B^{TES}	Binary variable of heating storage charge; equals 1 if heating storage is charged.
A^{ESS}	Binary variable of electricity storage discharge; equals 1 if electricity storage is discharged.
B^{ESS}	Binary variable of electricity storage charge; equals 1 if electricity storage is charged.
PCH^{ESS}	Power charge of ESS.
$PDCH^{ESS}$	Power discharge of ESS.
T_{Boiler}	Aggregated duration of compression chiller operation.
T_{ESS}	Aggregated duration of ESS operation.
T_{CHP}	Aggregated duration of CHP operation.
T_{TES}	Aggregated duration of TES operation.
t_0	Outside air temperature (°C).
$Trans \cup CHP\_Site$	The set of upward utility transformer and CHP sites.
QCH^{TES}	Heat charge of TES.
$QDCH^{TES}$	Heat discharge of TES.
W	Weight factor.
β	Present worth factor.
γ	Probability of contingency.
ψ	Binary decision variable of device installation (equals to 1 if device is installed).
δ	Duration of device operation.
$\chi_{\max}$	Maximum velocity of energy carrier in pipe (m/s).
$\kappa_{Purchased}^{Elect}$	Electricity purchasing price that is purchased from upward utility (MUs/kWh).
κ_{DLC}	Energy cost of DLC program (MUs/kWh).
κ_{Trans_price}	Transmission service price (MUs/kWh).
f	Maximum discharge coefficient of heating storage.
g	Maximum discharge coefficient of electricity storage.
$a_{CHP}^{th}, b_{CHP}^{th}, c_{CHP}^{'th}$	Coefficient of heat-power feasible region for CHP unit.
Ω	Small wind turbine blade angular velocity [rad/s].
η	Photovoltaic array conversion efficiency.
$\Delta\theta_{(input-output)}$	Temperature difference of input/output water (°C).
ζ	Specific heat capacity.

v_c^{Wind}	Small wind turbine cut-in wind velocity.
v_f^{Wind}	Small wind turbine cut-off wind speed.
ρ_{water}	Water density (kg/m3).
ϑ^{DRP}	Capacity fee for DRP.
ϖ^{DRP}	Active or reactive energy fee for DRP.
ξ^{DRP}	Allocated capacity of AIMG for DRP.

1. Introduction

The utilization of Distributed Energy Resources (DERs) and Demand Response Programs (DRPs) lead to complication of energy infrastructures expansion planning and operation. An Energy Distribution Company (EDC) may supply its downward MicroGrids (MGs) with energy carriers through its electric network and District Heating Network (DHN) [1]. The EDC may use Combined Heat and Power (CHP) systems, boilers and DRP to dispatch energy carriers. Industrial MG (IMG) may perform as an Active IMG (AIMG) that handles electricity with ascendant EDC [2]. Further, as shown in Fig. 1 the AIMGs can transact electricity with others through EDC's electric grid based on smart grid infrastructure [1].

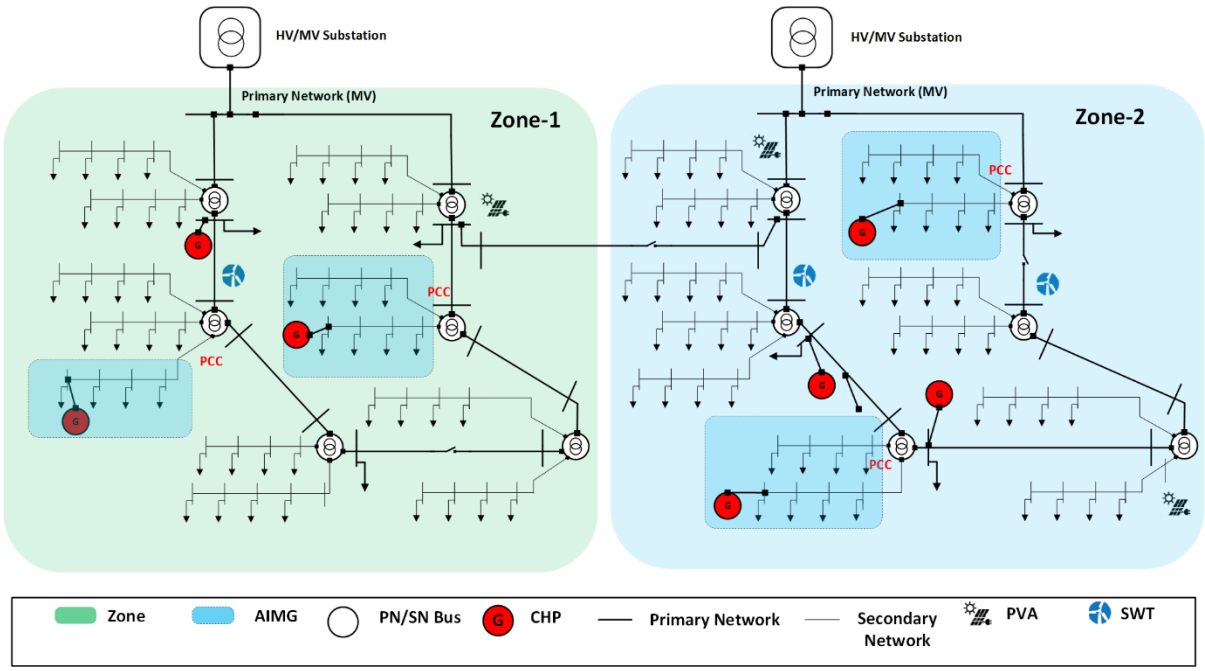

Fig. 1. Schematic diagram of an EDC with its AIMGs.

Distributed Cogeneration and Networks Expansion Planning (DCNEP) problem optimizes the parameters based on the cost-benefit analysis and reliability criterion [3, 4]. However, the electricity transaction between AIMGs must be investigated in the planning process based on the fact that the EDC operator can allow the AIMGs to transact electric energy with each other through its open accessed main grid [1].

Ref. [5] presented an integrated model including Small Wind Turbines (SWTs), Solar Photovoltaic Arrays (PVAs), heat pump, Electrical Storage Systems (ESSs), Thermal Storage Systems (TESs) and the algorithm used Mix Integer Linear Programming (MILP) optimization process to minimize energy costs and pollutant emissions. Ref. [6] introduced a linear optimization method for system planning of large-scale CHP units and it utilized a MILP algorithm to solve the formulated problem. The case study results revealed a 33% reduction in aggregated costs. Ref. [5, 6] didn't consider AIMG electricity transactions.

Ref. [7] presented an expansion-planning algorithm for the electric distribution system that was considered the uncertainties of load and wholesale market price. The introduced method utilized the harmony search method to minimize the aggregated costs of the system and the results were compared with the Genetic Algorithm (GA) and particle swarm optimization methods. This reference did not consider renewable DERs and AIMGs electricity transactions.

Ref. [8] introduced an optimization technique for the expansion planning of a district energy system considering the timing, type of capacity expansion, and operational modes. The dynamic optimization problem maximized the profitability of the system throughout the 30 years of the planning horizon. The optimization model considered the optimal economic, environmental, and regulatory constraints.

Ref. [9] presented the expansion planning optimization of electrical and thermal energy systems. A honeybee mating optimization algorithm was applied to minimize loss costs, voltage deviation and investment cost and the method was applied to two modified test systems. Ref. [8, 9] did not consider renewable DERs and AIMGs electricity transactions.

Ref. [10] investigated the methodology of expansion planning of district energy systems and evaluated the effectiveness of the proposed algorithm for the Ningbo Hi-Tech district in China was conducted. The results demonstrated that input energy, input exergy and Carbon dioxide (CO_2) emission were reduced by 22.7–24.1%, 14.5–14.9% and 5.9–6.6%, respectively.

Ref. [11] utilized composite indicators to assess the performances of a CHP plant in the planning procedure. The method was tested for a medium-size CHP-based district heating system. The results showed that the proposed method modified the operating strategies of system. Ref. [10, 11] did not consider renewable DERs and AIMGs electricity transactions.

Ref. [12] introduced a method for optimal district heating network expansion planning problem that used MILP approach to maximize cost-saving and minimize gas emissions. The proposed methodology was studied for different expansion planning scenarios of a real district heating system and the results showed that about 30% of costs were reduced. This reference did not model the AIMG electricity transactions and DER facilities.

Ref. [13] presented a mathematical model for district heating system planning that maximized revenues and minimized investment and operational costs. Different scenarios were considered for expansion planning of real energy system and results showed that the proposed algorithm reduced the aggregated costs about 33.11%.

Ref. [14] introduced a mathematical programming algorithm for optimal design and planning of a new district heating systems: energy reciprocity and on-site generation. The proposed algorithm minimized capital and operation costs and maximized the benefits of selling electricity to the grid. The model was assessed for a part of Suurstoffi district situated in Risch Rotkreuz, Switzerland and the results showed that the proposed method decreased about 25% in total annualized cost and 5% in emission compared to the conventional districts. Ref. [13] and [14] did not consider renewable DERs and AIMGs electricity transactions.

Ref. [15] presented a framework for finding the optimal district heating network layout and production technologies by considering renewable energy facilities. The proposed Mix Integer Non-Linear Programming (MINLP) model optimized the technical characteristics of the design and the case study on an existing DHN is presented. The results showed that the introduction of renewable energy into the energy mix was economically profitable and more than 15 % of the total cost was reduced.

Ref. [16] introduced an algorithm for the planning of gas/electricity/heat hybrid networks and hydrogen storage systems were used as an electricity storage system. A MILP algorithm was utilized to optimize the operation schedule of the system and minimize shed load. Further, a GA was also used to minimize the total investment costs. To model the contingencies, the worst-case scenario was explored. Two cases were tested and the results showed that the proposed method enhanced the utilization of DERs for different planning scenarios.

Ref [17], proposed a MILP procedure to find the optimal combinations of energy systems for an eco-town in the United Kingdom. The model minimized costs and the CO_2 emissions, but the AIMG electricity transactions and electric system contingencies were not modelled.

Ref [18], determined the optimal configuration and device capacity of the energy resource system. The algorithm minimized total costs of the energy system and a MILP optimization algorithm was utilized to find the optimality of the system topology and facilities, but the AIMG electricity transaction was not modelled.

Ref [19] introduced a MILP model for optimal planning of DERs systems that minimized energy costs and the model considered DERs, district heating system facilities, but the AIMG electricity transactions and system contingencies were not modelled. Ref [20], presented a MILP solution algorithm of CHP-based systems for Arenzani in Italy that optimized investment and operating costs. In Ref. [21], the expansion planning of microgrid was presented that maximizes the microgrid reliability and profit; meanwhile, it minimized operation and investment costs. Ref. [20] and [21] did not consider AIMGs electricity transactions.

The AIMGs' electricity transactions may have different time patterns, values and transactions locations that the evaluation of the feasibility and optimality of these transactions imposes a very heavy computational burden on the DCNEP procedure. An integrated model that considers the impact of the AIMGs' electricity transactions on the optimal expansion planning of distributed energy resources and networks is less frequent in the literature and is not presented in the available literature before, to the best of the authors′ knowledge.

Table 1 shows the comparative methodologies of proposed DCNEP algorithm. The main contributions of this paper are:

- The proposed algorithm considers the electricity transactions between the AIMGs and the EDC's loads on the DCNEP for the first time,
- The integrated model of DCNEP is proposed that considers the models of district heating and electric networks, intermittent renewable energy resources, thermal and electricity storage systems, CHPs, Direct Load Control (DLC) procedures, and electricity transactions between AIMGs in the planning and operational procedures,
- The proposed stochastic model considers four sources of system uncertainties that consist of the intermittent power generations, AIMGs' energy consumptions, AIMGs' electricity transaction, and the system contingencies,
- The overall framework and solution methodology of the proposed heuristic three-stage algorithm is another contribution of this research that considers the optimal coordination of EDC's energy resources in normal and contingent condition.

2. Problem Modelling and Formulation

As shown in Fig.2, the EDC operator utilizes its CHP systems and boilers to supply the downward heat and electricity loads and it can purchase electricity from the upward wholesale market. Further, the electricity surplus of each AIMG can be sold to the EDC or transacted to other AIMG and/or other loads. Any AIMGs' electricity transactions must be approved by the EDC in advance. The EDC is equipped with different energy resources consists of gas-fired CHPs and boilers, PVAs, SWTs, ESSs, and TESs. The DCNEP must minimize the investment and operation cost; meanwhile, it must maximize the reliability of provided services for the downward heating and electrical loads [22].

Table 1: Comparison of proposed DCNEP with other researches.

References		5	6	7	8	9	10	11	12	13	14	15	16	17	18	19	20	21	Proposed Approach
Method	MILP	✓	✓	×	×	×	×	×	✓	×	✓	×	×	✓	✓	✓	✓	×	×
	MINLP	×	×	×	✓	×	✓	✓	×	×	×	✓	×	×	×	×	×	×	×
	Heuristic	×	×	✓	×	✓	×	×	×	✓	×	×	✓	×	×	×	×	✓	✓
	Deterministic	✓	×	×	×	×	✓	✓	✓	✓	✓	✓	×	✓	✓	✓	✓	×	×
	Stochastic	×	✓	✓	✓	✓	×	×	×	×	×	×	✓	×	×	×	×	✓	✓
Objective Function	Revenue	×	×	×	×	×	×	×	×	×	×	×	×	×	×	✓	×	×	✓
	Generation cost	✓	✓	✓	✓	✓	✓	✓	✓	✓	✓	✓	✓	✓	✓	✓	✓	✓	✓
	Storage cost	✓	×	×	×	×	✓	×	✓	×	×	✓	×	✓	✓	×	✓	✓	✓
	Electric system contingency costs	×	✓	×	×	×	×	×	×	✓	×	×	×	×	×	×	×	✓	✓
	AIMG electricity transactions benefits	×	×	×	×	×	×	×	×	×	×	×	×	×	×	×	×	×	✓
	DLC benefits	×	×	×	×	×	×	×	×	×	×	×	×	×	×	×	×	×	✓
	SWT costs	✓	×	×	×	×	×	×	×	×	×	×	×	✓	×	×	✓	✓	✓
	PVA costs	✓	×	×	×	×	✓	×	×	×	✓	×	✓	✓	×	×	✓	✓	✓
Nonlinear feasible operating region of CHP unit		✓	✓	×	×	×	✓	×	×	✓	×	✓	✓	✓	✓	✓	×	×	✓
Storage System	EES	✓	✓	×	×	×	✓	×	×	×	×	×	×	×	×	×	✓	✓	✓
	TES	✓	✓	×	×	×	×	×	×	×	×	×	✓	×	×	×	×	×	✓
Constraints of AIMG electricity transactions		×	×	×	×	×	×	×	×	×	×	×	×	×	×	×	×	×	✓
Grid Connected		✓	✓	✓	✓	✓	✓	✓	✓	✓	✓	✓	✓	✓	✓	✓	✓	✓	✓
Expansion planning of electric system		×	×	×	×	×	×	×	×	×	×	×	×	×	×	×	✓	✓	✓
Expansion planning of district heating system		×	×	×	×	×	✓	×	×	✓	✓	✓	×	×	×	×	×	×	✓
Simultaneous expansion planning of electric and district heating systems		×	×	×	×	×	×	×	×	×	×	×	×	×	×	×	×	×	✓

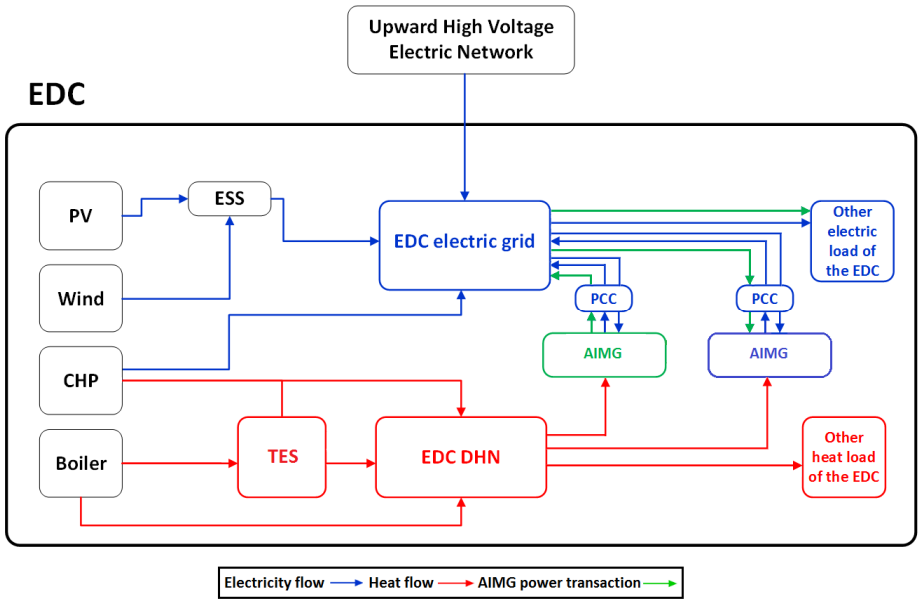

Fig. 2. The EDC energy resources and storages.

2.1. Uncertainty modelling

The DCNEP problem is subject to the four uncertainty causes: The intermittent power generation of the EDC, AIMG's energy consumption scenarios, AIMGs' electricity transaction scenarios, and the system contingencies, as shown in Fig.3.

An AIMG can be supplied by heating and electricity energy through the EDC's DHN and electricity grid, respectively. The uncertainty modelling is performed in a three-stage procedure. The AIMG can request from the upward EDC to deliver its injected electricity to other AIMGs through the EDC's main grid. The EDC must consider the uncertainties of the AIMGs' electricity transactions. The EDC uses an estimated data of hourly electric and heat loads and its intermittent electricity generations for each year of planning years, AIMGs' energy consumptions scenarios and electricity transaction location, quantity and electricity flow direction. The EDC estimates the optimal generation schedules of its generation units, electricity transactions with the upward wholesale market and AIMGs, estimated DRPs control variables and contingency-based load shedding alternatives. Thus, a three-stage stochastic optimization program can be utilized. At the first stage problem, the DCNEP determines the initial location and capacity of electric and heating systems for each AIMG's energy consumption scenario. At the second stage problem, the feasibility of estimated AIMGs' electricity transactions are evaluated and the optimal scheduling of the EDC's CHPs and energy resources in normal states are determined. Finally, at the third stage problem, DRPs alternatives, load shedding and the AIMGs' electricity transaction interruptions for contingent conditions are decided. The three-stage procedure is repeated until the stopping criterion is satisfied.

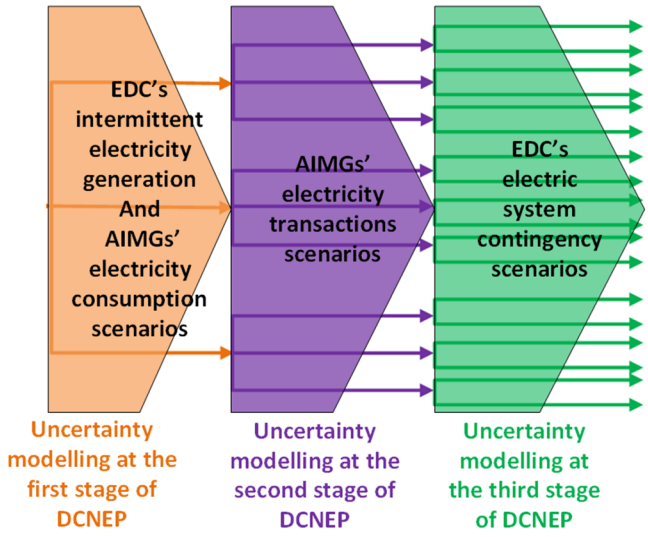

Fig. 3. Three-stage scenario-based model for DCNEP.

2.2. DRP modelling

The AIMG load is categorized into critical and controllable loads [23]. Thus, the AIMG controllable loads can be dispatched by the EDC in the DLC program [24, 25]. The EDC can utilize the DLCs program in normal and/or contingent conditions that change the commitment of its DERs [26-28]. The EDC can pay capacity and energy fees to the AIMGs to participate in DRPs. Thus, the DRP costs can be formulated as (1) [29, 30]:

$$TC_{DRP} = \sum_{NDRP} \vartheta^{DRP}.\xi^{DRP} + \varpi^{DRP}_{Active}.P^{DRP} + \varpi^{DRP}_{Reactive}.Q'^{DRP} \quad (1)$$

The TC_{DRP} consists of DRP capacity fee, active power and reactive power fees that are paid by the EDC to the DRPs that contribute in the DLC programs.

2.3. First Stage Problem Formulation

The DCNEP minimizes total investment and operation costs and maximizes the system reliability. The decision variables of the first stage problem are the location, capacity and time of installation of the EDC's facilities. The EDC facilities are CHPs, electric feeders, DHN pipes, PVAs and SWTs, ESSs, TESs, boiler and switching devices. The purchasing cost of energy purchased from the upward market, DRP costs, interruption cost of customers and the benefit of AIMGs' electricity transactions should be considered in the optimization process. Thus, the objective function of the first stage problem for the entire of the planning horizon can be formulated as (2):

$$Min\ \mathbf{R}_1 = \sum_{Nyear}\sum_{Nzone}\sum_{NOIS} prob \times \begin{pmatrix} (TC_{CHP}.\psi^{CHP} + TC_{Feeder}.\psi^{Feeder} + TC_{Pipe\_DHN}.\psi^{Pipe\_DHN} + \\ +TC_{PVA}.\psi^{PVA} + TC_{SWT}.\psi^{SWT} + TC_{ESS}.\psi^{ESS} + TC_{TES}.\psi^{TES} + \\ TC_{Boiler}.\psi^{Boiler} + TC_{SW}.\psi^{SW}) + TC_{IC} + TC_{Purchase} + TC_{DRP} \\ -TB_{PT} \end{pmatrix} \quad (2)$$

The *NOIS* parameter presents the total number of AIMG's energy consumption scenarios and the EDC's intermittent electricity generation and its corresponding probability is presented as *prob* parameter. The objective function can be decomposed into five groups: 1) the investment plus aggregated operation costs of CHP, electric feeder, DHN pipe, PVA, SWT, ESS, TES, boiler, and switching device, 2) The interruption cost of electric system contingency, 3) the energy purchased costs, 4) the costs of DRPs and 5) the benefit of electricity transactions of AIMGs.

The 3rd, 4th, and 5th group of objective functions are calculated at the second stage problem. The 2nd group of the objective function is calculated at the 3rd stage problem.

The energy resource investment costs consist of annualized fixed costs and variable costs. The variable cost is a function of operation time and maintenance cost, operation cost, and emissions cost. Thus, the facilities investment and aggregated operation costs can be written as (3-8):

$$TC_{CHP} = \beta.\sum_{CHP\_Site}\sum_{CHPC}(TC^{CHP}_{Invest} + \sum_{NOSS} prob.\sum_{T_{CHP}}\delta.(TC^{CHP}_{Op} + TC^{CHP}_{M} + TC^{CHP}_{EM})) \quad (3)$$

$$TC^{CHP}_{EM} = \sum EM^{CHP}_{X''}.EMC_{X''} \qquad \forall X'' \in \{CO_2,\ SO_2,\ NO_X\} \quad (4)$$

$$TC_{Boiler} = \beta.\sum_{Boiler\_Site}\sum_{BC}(TC^{Boiler}_{Invest} + \sum_{NOSS} prob.\sum_{T_{Boiler}}\delta.(TC^{Boiler}_{Op} + TC^{Boiler}_{M} + TC^{Boiler}_{EM})) \quad (5)$$

$$TC^{Boiler}_{EM} = \sum EM^{Boiler}_{X'''}.EMC_{X'''} \qquad \forall X''' \in \{CO_2,\ SO_2,\ NO_X\} \quad (6)$$

$$TC_{ESS} = \left(\beta . \sum_{ESS\_Site} \sum_{ESSC} (TC_{Inv}^{ESS} . Cap^{ESS} + \sum_{NOSS} prob. \sum_{T_{ESS}} \delta . (TC_{Op}^{ESS} + TC_{M}^{ESS})) \right) \quad (7)$$

$$TC_{TES} = \left(\beta \times \sum_{TES\_Site} \sum_{TESC} (TC_{Inv}^{TES} . Cap^{TES} + \sum_{NOSS} prob. \sum_{T_{TES}} \delta . (TC_{Op}^{TES} + TC_{M}^{TES})) \right) \quad (8)$$

The *EM* and *EMC* parameters are the pollutant emission and emission costs, respectively.

The DHN pipeline installation and electric feeder costs are the functions of their capacity and the length of the routing path. Thus, the electric feeder cost and DHN pipe cost can be written as (9-11):

$$TC_{Feeder} = \sum_{Trans \cup CHP\_Site} \sum_{Load\_Site} \beta . L. \left((TC_{Capacity}^{Feeder} . Cap^{Feeder} + TC_{leng}^{Feeder}) \right) \quad (9)$$

$$TC_{Pipe\_DHN} = \sum_{DH\_Site} \sum_{HL\_Site} \beta . L. \left((TC_{Capacity}^{DH} . Cap^{DH} + TC_{leng}^{DH}) \right) \quad (10)$$

$$Cap^{DH} = \rho_{water} . \pi . \left(R^{DHN} \right)^2 . \zeta . \chi_{\max} . \Delta\theta_{(input-output)} \quad (11)$$

The total interruption cost is the function of the shed electrical energy and the Composite Damage Function (CDF) of the electrical load.

$$TC_{IC} = \sum_{NOCS} \gamma . P_{shed} . CDF \quad (12)$$

The PVA and SWT costs are given by (13) and (14):

$$TC_{PVA} = \beta . \sum_{PVA\_Site} (TC_{Inv}^{PVA} . S_i^{PVA} + TC_{M}^{PVA}) \quad (13)$$

$$TC_{SWT} = \beta . \sum_{SWT\_Site} (TC_{Invest}^{SWT} + TC_{M}^{SWT}) \quad (14)$$

The benefit of electricity transaction of AIMG is a function of the value of the transacted power and the price of electricity transmission service and can be written as:

$$TB_{PT} = P_{PT} . \kappa_{Trans\_price} \quad (15)$$

The electric power balance constraint is given by (16):

$$P^{EDC} = (- \sum_{Load\_site} P^{Load} + \sum_{PVA\_Site} P^{PVA} + \sum_{ESS\_Site} P^{ESS} + \sum_{SWT\_Site} P^{SWT} + \sum_{CHP\_Site} P^{CHP} + \sum_{DRPA} P^{DRP} - P^{Loss}) \quad (16)$$

The energy purchased costs are given by:

$$TC_{Purchase} = P^{EDC} \times \kappa_{Purchased}^{Elect} \quad (17)$$

The heating power balance constraint is given by (18):

$$-\sum_{n\in Load\_site} Q_n^{Load} + \sum_{e\in Boiler\_Site} Q_e^{B} + \sum_{a\in CHP\_Site} Q_a^{CHP} - Q^{Loss} + \sum_{m'\in DH\_Site} \sum_{n\in Load\_site} Q_{m'n}^{Flow} = 0 \quad (18)$$

1 *A. TES and ESS constraints:*

2 TES maximum capacity:

$$Q^{TES} \le Cap^{TES} \quad (19)$$

3 TES maximum discharge and charge constraints:

$$QDCH^{TES} \le (f.Cap^{TES}).A^{TES} \qquad A^{TES} \in \{0,1\} \quad (20)$$

$$QCH^{TES} \le Cap^{TES}.B^{TES} \qquad B^{TES} \in \{0,1\} \quad (21)$$

4 TES cannot discharge and charge at the same time:

$$A^{TES}(t) + B^{TES}(t) \le 1 \quad \forall\ t\ ,\ A^{TES}\ and\ B^{TES} \in \{0,1\} \quad (22)$$

5 ESS maximum capacity:

$$P^{ESS} \le Cap^{ESS} \quad (23)$$

6 ESS maximum discharge and charge constraints:

$$PDCH^{ESS} \le (g.Cap^{ESS}) \times A^{ESS} \qquad A^{ESS} \in \{0,1\} \quad (24)$$

$$PCH^{ESS} \le Cap^{ESS}.B^{ESS} \qquad B^{ESS} \in \{0,1\} \quad (25)$$

7 ESS cannot discharge and charge at the same time:

$$A^{ESS}(t) + B^{ESS}(t) \le 1 \quad \forall\ t\ ,\ A^{ESS}\ and\ B^{ESS} \in \{0,1\} \quad (26)$$

8 *B. SWT and PVA constraints:*

9 SWT electricity generation is given by [31, 32]:

$$P^{SWT} = \begin{cases} 0 & if\ v^{Wind} \le v_c^{Wind}\ or\ v^{Wind} \ge v_f^{Wind} \\ P_r^{Wind}.\dfrac{(v^{Wind} - v_c^{Wind})}{(v_r^{Wind} - v_c^{Wind})} & if\ v_c^{wind} \le v^{Wind} \le v_r^{wind} \\ P_r^{Wind} & otherwise \end{cases} \quad (27)$$

10 The minimum noise disturbance constraint is considered as [33]:

$$L_P \approx 50.\log_{10}.\Omega.R^{SWT} + 10.\log_{10}.R^{SWT} - 1 \quad (28)$$

11
12

13 The maximum electricity output of PVA is given by [34]:

$$\mathrm{P^{PV}} = S^{PVA}\eta I(1 - 0.005(t_0 - 25)) \quad (29)$$

14
15
16

B. DHN constraints:

The DHN is modelled as [35] and the DHN constraints consist of device and pipe loading constraints and flow direction constraints. The DHN flow constraints are given by (30):

$$Q_{Min}^{Flow} \le Q^{Flow} \le Q_{Max}^{Flow} \tag{30}$$

C. CHP constraints:

Nonlinear feasible operating region for CHP units:

$$a_{CHP}^{th}.P^{CHP} + b_{CHP}^{th}.Q^{CHP} \ge c'^{th}_{CHP} \tag{31}$$

$$P_{Min}^{CHP} \le P^{CHP} \le P_{Max}^{CHP} \tag{32}$$

$$Q_{Min}^{CHP} \le Q^{CHP} \le Q_{Max}^{CHP} \tag{33}$$

D. Boiler constraints:

Heat output limit for boilers:

$$Q_{Min}^{B} \le Q^{B} \le Q_{Max}^{B} \tag{34}$$

E. DRP constraints:

Based on the DRP modelling section, the DRP constraints can be written as [36-44]:

$$P^{Load} = P_{Critical}^{Load} + P_{Controllable}^{Load} \tag{35}$$

$$\Delta P_{Min}^{DLC} \le \Delta P^{DLC} \le \Delta P_{Max}^{DLC}\ ,\ \Delta P_{Max}^{DLC} = P_{Controllable}^{Load} \tag{36}$$

$$P^{DRP} = \Delta P^{DLC} \tag{37}$$

$$TC_{DRP} = P^{DRP}.\kappa_{DLC} \tag{38}$$

F. Electric network constraints:

The electric device loading constraints and the DC load flow constraints must be considered in the 1st stage of optimization.

The integrated constraints of the first stage optimization problem can be represented as:

$$Z_1(x,u,z) = 0 \tag{39}$$

$$\Upsilon_1(x,u,z) \le 0 \tag{40}$$

where, *x, u, z* are problem variables, controls and system topology, respectively.

2.4. Second Stage Problem Formulation

The second stage problem optimizes the operational subproblem of DCNEP and it minimizes the operation costs of system resources in the normal conditions that can be represented as:

$$Min\ \mathbf{R}_2 = \sum_{NOSS} prob. \sum_{Nzone} \begin{pmatrix} TC_{Op}^{CHP} + TC_{Op}^{Boiler} + TC_{Op}^{ESS} + TC_{Op}^{TES} + \\ TC_{Purchase}^{Up} + TC_{DRP} - TB_{PT} \end{pmatrix} \quad (41)$$

$$s.t.: \quad Z_2(x,u,z) = 0$$
$$\Upsilon_2(x,u,z) \le 0$$

Where, $Z_2(x,u,z)=0$ and $\Upsilon_2(x,u,z)\le 0$ are second stage problem constraints.

2.5. Third Stage Problem Formulation

At the third stage problem, the optimal operational coordination of the EDC's resources for the contingent condition is assessed. The third stage problem objective function minimizes the mismatch of the 2nd stage optimal dispatch costs plus the total interruption costs.

The objective function of the third stage problem can be represented as:

$$Min\ \mathbf{R}_3 = \sum_{NOSS} prob. \sum_{NCCS} prob. \sum_{Nzone} \begin{pmatrix} \Delta TC_{Op}^{CHP} + \Delta TC_{Op}^{Boiler} + \Delta TC_{Op}^{ESS} + \Delta TC_{Op}^{TES} + \\ \sum_{Ncont} \gamma . P_{shed} . CDF - \Delta TB_{PT} \end{pmatrix} \quad (42)$$

$$s.t.: \quad Z_3^{'\alpha}(x,u,z) = 0 \qquad \forall \alpha \in \{0,1,....,NCSS\}$$
$$\Upsilon_3^{'\alpha}(x,u,z) \le 0$$

Where, $Z_3^{'\alpha}(x,u,z)=0$ and $\Upsilon_3^{'\alpha}(x,u,z)\le 0$ are the detailed AC power flow model of $Z_2(x,u,z)=0$ and $\Upsilon_2(x,u,z)\le 0$, respectively.

The general form of the first, second and third stage can be rewritten as the following equation:

$$\boldsymbol{Max}\ \mathbf{R}_i^{'} = \boldsymbol{M}' - \mathbf{R}_i - \boldsymbol{W}.Z_i(\boldsymbol{u},\boldsymbol{x},\boldsymbol{z}) - \boldsymbol{W}'.\Upsilon_i(\boldsymbol{u},\boldsymbol{x},\boldsymbol{z}) \qquad \forall\ \boldsymbol{i}\ \in \{\text{First, second and third stages}\} \quad (43)$$

Where, $\mathbf{R}^{'}$ and *M'* are objective function and high number vectors, respectively. *W* and *W'* are weight factor vectors.

3. Solution Methodology

The proposed DCNEP is an MINLP problem that has multiple discrete and continuous variables in the planning and operational subproblems. The subproblems are the optimal power flow of energy systems in normal and contingent condition of systems [45]. The authors attempted to define a proper framework to solve the DCNEP problem and different framework and soft computing results were compared, and finally, the proposed framework was selected. The overall solution methodology is one of the contributions of this paper that tries to trade-off between accuracy and computational complexity.

Further, the AIMGs' electrical transactions may have different time patterns, values and transactions locations. The evaluation of the feasibility and optimality of these transactions imposes a very heavy computational burden on the DCNEP procedure that may lead to custom MINLP algorithms divergence and/or memory overflow. Thus, an iterative three-stage optimization algorithm is proposed and Fig. 4 depicts the flowchart of the optimization algorithm. The flowchart blocks are presented in the following paragraphs.

For the first, second and third stage optimization problems, an Integrated Adaptive Genetic Algorithm (IAGA) with variable fitness functions is used to find the feasible solution of the modelled large-scale MINLP problem.

The IAGA dynamically changes the values of mutation and crossover probability to overcome this problem. Further, it changes the type of crossover of the algorithm [46, 47]. It uses a deterministic and reinforcement-based algorithm to modify the operators' values and the most valuable parameters of GA are rewarded and reinforced. Then, the rewarded parameters are applied in the subsequent generation of chromosomes. The best solution of each IAGA population is protected and the crossover operator cannot change it and zero or minimum value of mutation operator is applied to the protected solutions. The detailed explanation of IAGA is available in [46-47].

At the first stage problem, the hourly electrical and thermal load data are transformed into Quarterly Load Duration Curves (QLDCs) that present the fixed values of electrical and thermal energy demands for each quarter of the planning year. It is assumed that the first-stage candidate facilities are working at their maximum capacity and their installation variables are presented as the continuous variables. Then, a list of the feasible candidates of the installation facilities is selected and the problem constraints are considered as penalty factors in the objective function. The IAGA is implemented and multiple solutions are obtained and all of the feasible solutions are saved and explored in the next stages.

At the second and third stages, the hourly energy load curves are used to assess the operational condition of selected first stage decision variables. For the second stage problem, for all of the feasible solution of fist stage problem, the list of all of the AIMGs' electricity transactions to other AIMGs and/or other loads are generated and their feasibility and optimality are evaluated by the second stage objective function and the feasible and optimal electricity transactions are selected. At the third stage problem, the optimization problem explores the detailed optimal operation of energy systems in contingent conditions for each of the second stage problem outputs. The third stage problem simulates the outage of the electric system components and it tries to find the optimal coordination of system resources. If the electrical system resources are not adequate to supply the electrical load, then the following algorithm is performed: At first, the controllable loads are switched off and the DLC procedure is performed. Then, the zonal load block and the corresponding electricity transactions of AIMGs are cancelled. At the final step of the third stage problem, the involuntary load shedding is performed. The three-stage procedure is repeated until the stopping criterion is satisfied.

The Modified Weighted Reliability Index (MWRI) is used for stopping criterion, defined as:

$$MWRI = wf'_1.SAIDI + wf'_2.SAIFI + wf'_3.ENSC \quad (44)$$

Where,

$$SAIFI = \text{Total number of system interruptions/ total number of the EDC's zones served.} \quad (45)$$

$$SAIDI = \text{Sum of the interruption duration / total number of the EDC's zones.} \quad (46)$$

$$ENSC = \text{Energy not supplied cost.} \quad (47)$$

wf'_1, wf'_2, wf'_3 are the weight factor vectors.

4. Simulation Results

Three systems are used to assess the proposed DCNEP algorithm. The 9-bus, 33-bus and 123-bus IEEE test systems are considered.

A. 9-bus test system

The 9-bus test system data is presented at [48] and its topology is shown in Fig.5. The proposed DCNEP algorithm was assessed by the full search algorithm and the results of the proposed and full search algorithms are presented in the following paragraphs. The value of the first stage uncertainty modelling was assumed as NOIS=2 to reduce the whole state-space of the full search algorithm. Fig. 6 depicts the electrical and heating peak load forecasting for the base case (first scenario of NOIS).

The wind turbine and solar panel data are available at [49]. Fig.7 depicts the hourly heating and electrical loads of the 9-bus test system for the final planning year. Fig. 8. shows the forecasted market price for the base year. Table A1, Table A2, and Table A3 of the appendix present the characteristics of CHPs, conductors and DCNEP parameters for the 9-bus test system, respectively. Table A4 of the appendix presents the DERs, DHN, DRP and emission data for all of the case studies.

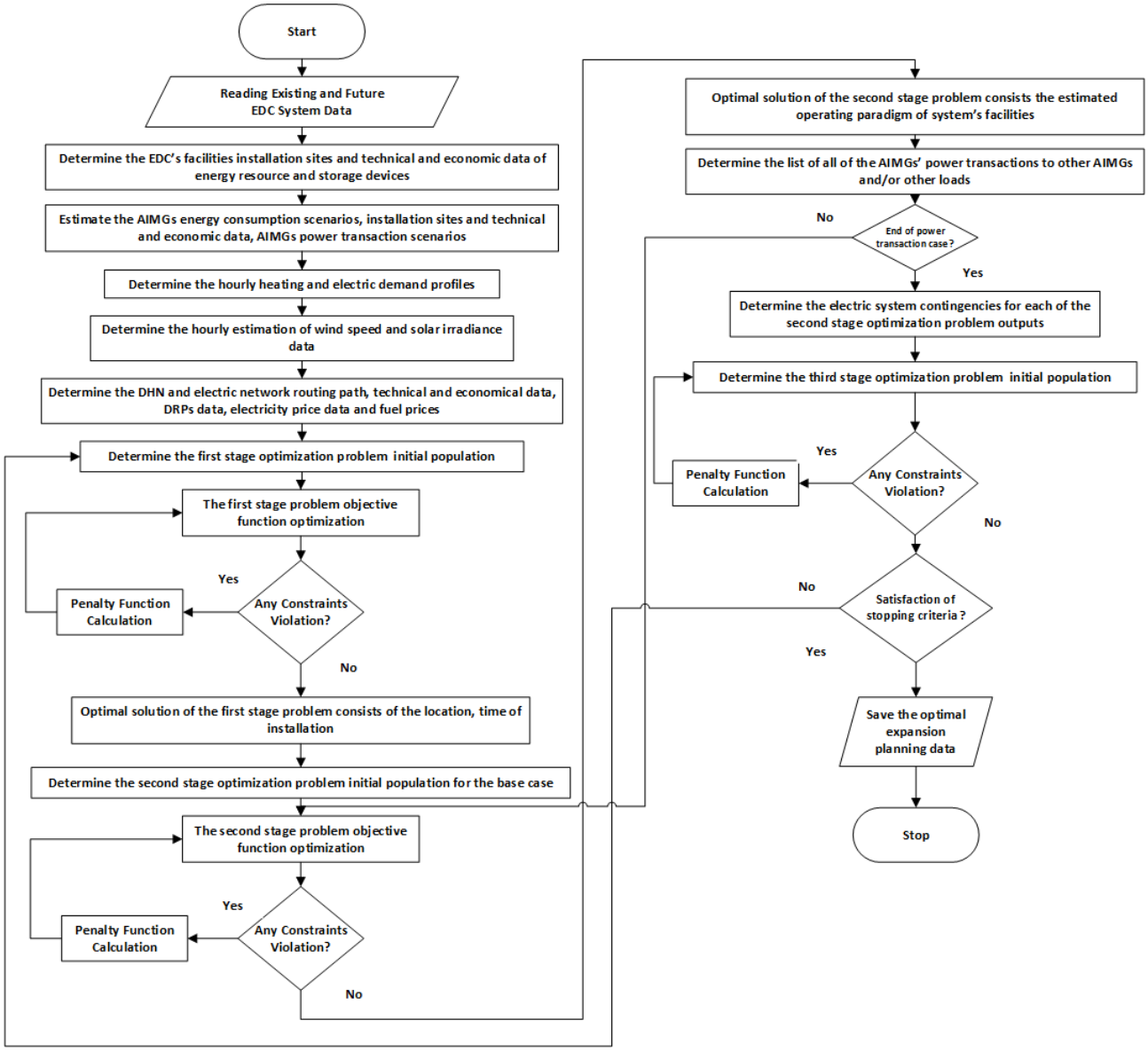

Fig. 4. Flowchart of the DCNEP algorithm.

The DCNEP problem subjects to the three sources of uncertainty:

1) AIMG's energy consumption scenarios are the first source of uncertainty. The yearly and hourly energy consumptions for NOIS=1 are depicted in Fig. 6 and Fig.7, respectively. For the NOIS=2, the parameters of NOIS=1 are multiplied by 0.7,
2) The AIMGs' electricity transaction scenarios. The EDC must simulate the feasibility and optimality of the probable AIMGs' electricity transactions.
3) The system contingencies. The forced outage rate data were used to simulate the 9-bus contingencies.

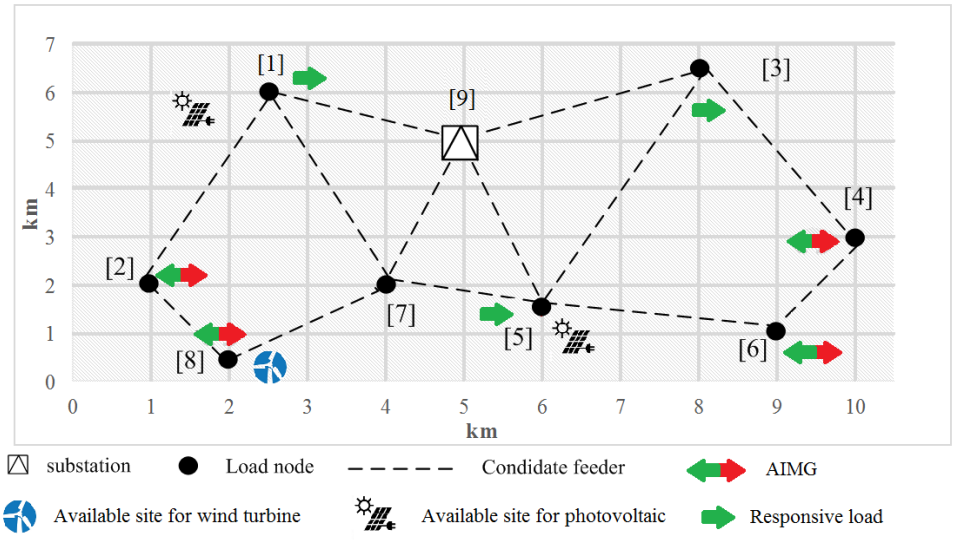

Fig. 5. The 9-bus distribution network.

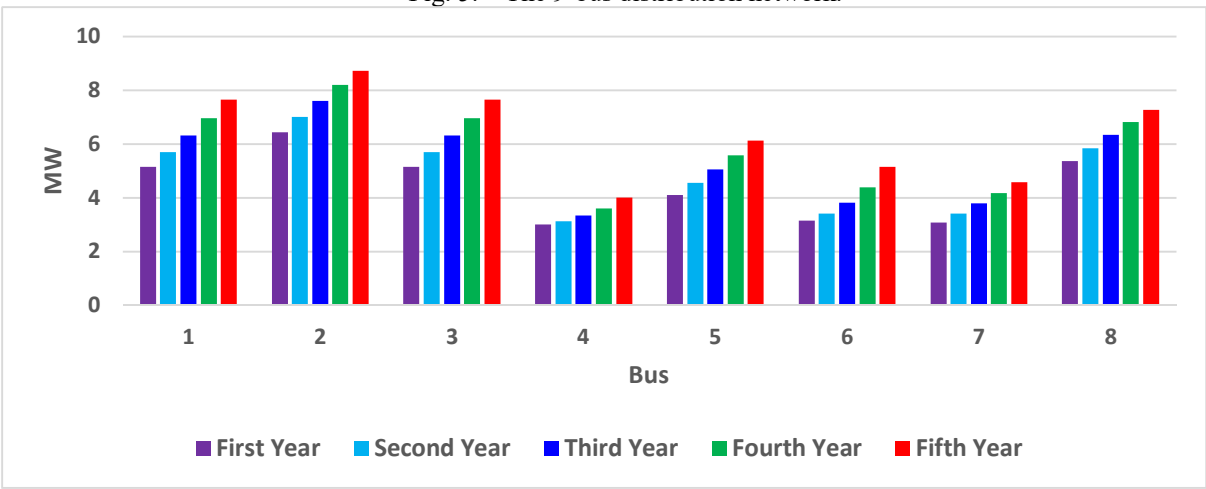

Fig. 6. Five-year peak load forecasting for the electrical and heating loads of the 9-bus test system.

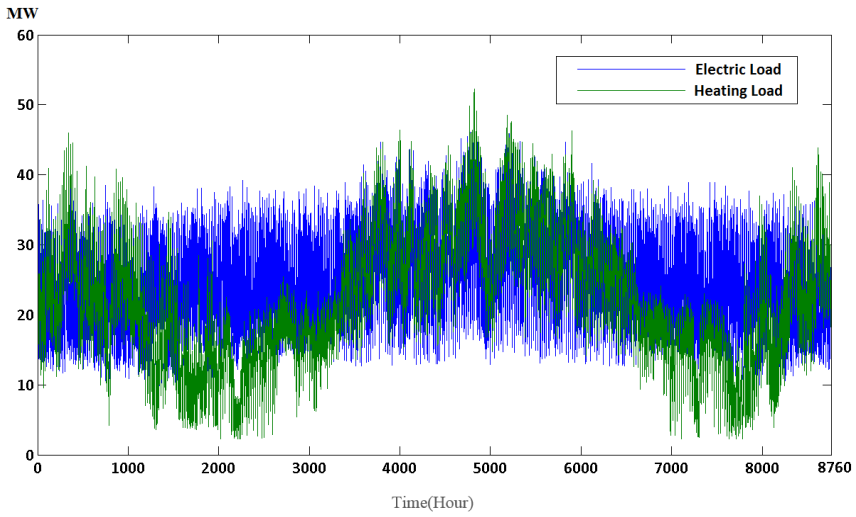

Fig.7. Hourly thermal and electrical load of the 9-bus system for the final year of the planning horizon.

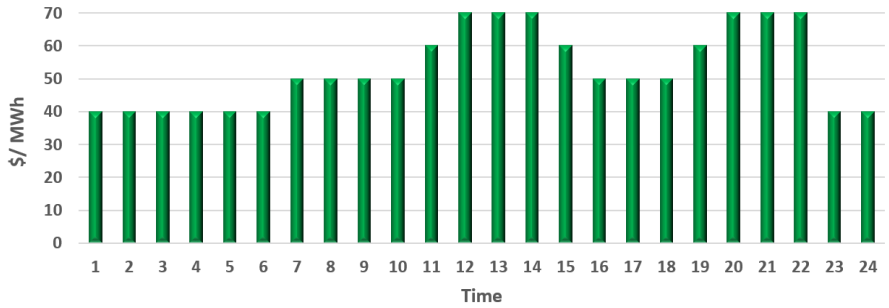

Fig.8. Hourly electricity market price for the 9-bus system for the first year of the planning horizon.

The AIMG can request from the upward EDC to deliver its electricity to other AIMGs through the EDC's main grid. Thus, the EDC must simulate the uncertainties of the AIMGs' electricity transactions. The EDC prepares the list of the AIMGs' electricity transactions and explores the feasibility of the transactions. Different electricity transaction blocks can be modelled by the different steps of power injections and withdrawals into/from electric system buses that are formulated by the load flow equations. For the 9-bus test system, the electricity transaction block is selected as the 0.1 MW step. Table 2 presents the feasible and optimum AIMGs' electricity transaction cases for the electric load peak condition. The optimal value of electricity transaction is shown in green.

Table 2. The 9-bus system feasible and optimum AIMGs' electricity transaction cases.

	Bus 1	Bus 2	Bus 3	Bus 4	Bus 5	Bus 6	Bus 7	Bus 8
Bus 2	4.2125 MW	-	0.1572 MW	0.1712 MW	x	4.3401 MW	x	2.7198 MW
Bus 4	3.3188 MW	x	7.5 MW	-	3.4762 MW	x	x	x
Bus 6	3.3212 MW	x	0.1628 MW	x	7.5 MW	-	2.9563 MW	x
Bus 8	3.3156 MW	x	0.1509 MW	x	3.4621 MW	3.4762 MW	7.5 MW	-

The optimal electric system and DHN topologies of the 9-bus test system for different years of expansion planning horizon are depicted in Fig. 9. The DCNEP installed the maximum available capacity of PVAs, SWTs and ESSs in the first year of planning.

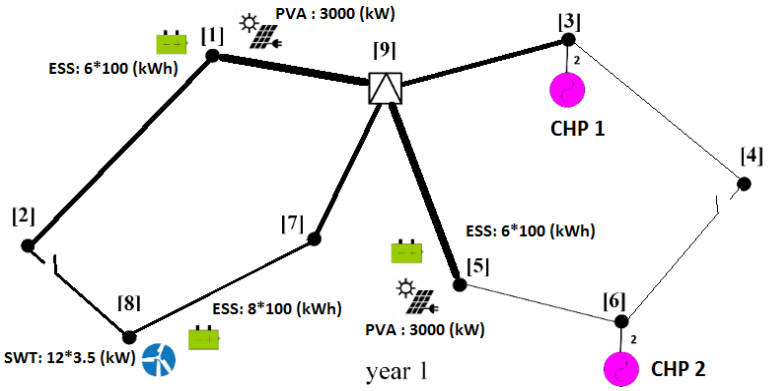
PVA : 3000 (kW)
[1]
ESS: 6*100 (kWh)
[9]
[3]
CHP 1
[4]
[2]
[7]
ESS: 6*100 (kWh)
[5]
[8]
ESS: 8*100 (kWh)
PVA : 3000 (kW)
[6]
SWT: 12*3.5 (kW)
CHP 2
year 1

(a)

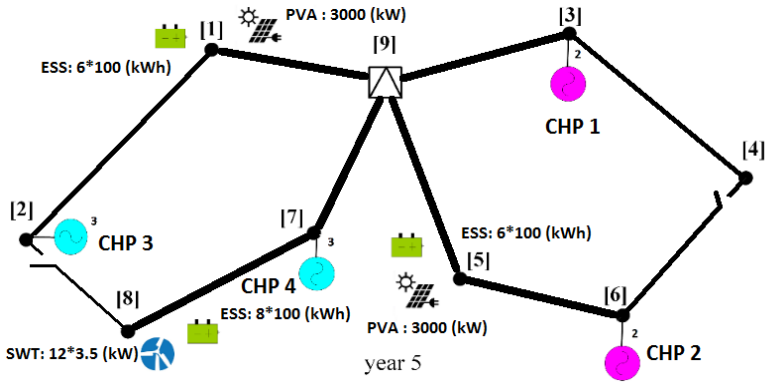
PVA : 3000 (kW)
[1]
ESS: 6*100 (kWh)
[9]
[3]
CHP 1
[4]
[2]
CHP 3
[7]
ESS: 6*100 (kWh)
[5]
CHP 4
[8]
ESS: 8*100 (kWh)
PVA : 3000 (kW)
[6]
SWT: 12*3.5 (kW)
CHP 2
year 5

(b)

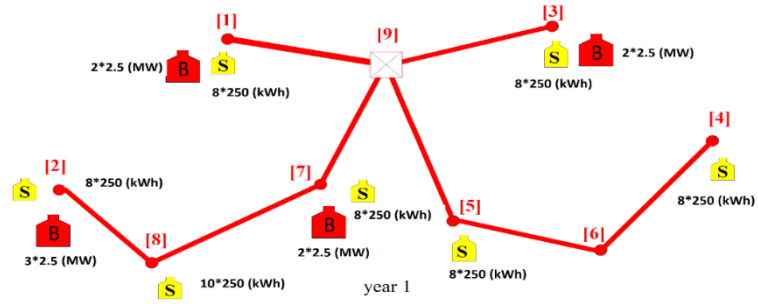
[1]
[9]
[3]
2*2.5 (MW)
8*250 (kWh)
2*2.5 (MW)
8*250 (kWh)
[4]
[2]
8*250 (kWh)
[7]
8*250 (kWh)
[5]
8*250 (kWh)
3*2.5 (MW)
[8]
[6]
2*2.5 (MW)
10*250 (kWh)
8*250 (kWh)
year 1

(c)

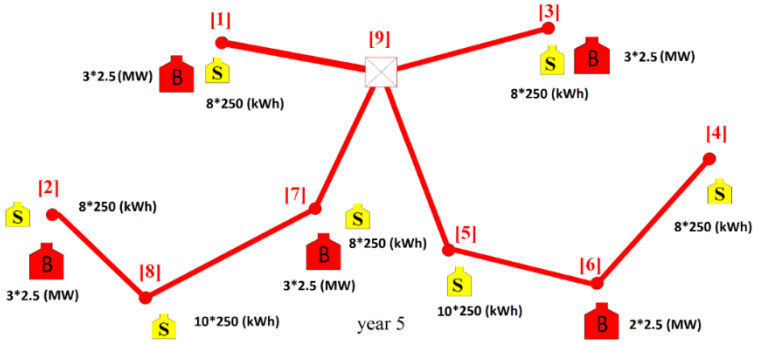
[1]
[9]
[3]
3*2.5 (MW)
8*250 (kWh)
3*2.5 (MW)
8*250 (kWh)
[4]
[2]
8*250 (kWh)
[7]
8*250 (kWh)
[5]
8*250 (kWh)
3*2.5 (MW)
[8]
[6]
3*2.5 (MW)
10*250 (kWh)
10*250 (kWh)
2*2.5 (MW)
year 5

(d)

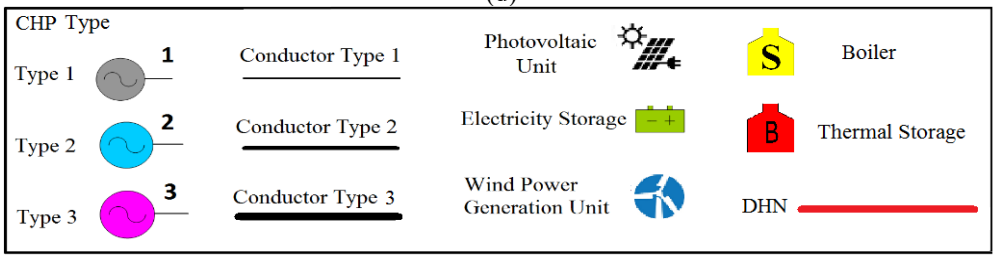
CHP Type
Type 1
1
Conductor Type 1
Photovoltaic Unit
Boiler
Type 2
2
Conductor Type 2
Electricity Storage
Thermal Storage
Type 3
3
Conductor Type 3
Wind Power Generation Unit
DHN

Fig. 9. (a) The optimal electrical system topology of the 9-bus test system for the 1st year of expansion planning horizon, (b) The optimal electrical system topology of the 9-bus test system for the 5th year of expansion planning horizon. (c) The optimal DHN topology of the 9-bus test system for the 1st year of expansion planning horizon, (d) The optimal DHN topology of the 9-bus test system for the 5th year of expansion planning horizon.

As shown in Fig. 9, the DCNEP installed the maximum capacity of the available intermittent DERs and ESSs. Further, the algorithm installed the maximum values of boiler facilities in the first year of the planning horizon. The district heating network was installed in the first year for all of the heating load buses and its parameters were not changed for the planning horizon. However, the algorithm installed the maximum capacity of TESs for the first year of the planning horizon based on the fact that TESs improved the ability of the EDC to handle the DRP programs and interruption of the AIMGs electricity transactions. The DCNEP gradually increased the capacity of installed CHP facilities based on the electrical load grow parameters. At the final year of expansion planning, more CHPs were installed to supply the customers.

Table 3 depicts the optimal outputs of DCNEP for the 9-bus test system. One of the main purchasing cost of the system was natural gas purchasing costs that took on a value 36.2514 MMUs.

Table 3. The optimal outputs of DCNEP for the 9-bus test system.

Costs (MMUs)			
Feeders installation costs	4.1514	Transformers and feeders operation costs	4.215
Transformer and ESS installation costs	9.2102	CHP installation and operation costs	26.8213
ENSCs	0.39265	Energy loss costs	0.75723
PVA installation and maintenance costs	4.2315	Wind turbine installation and maintenance costs	3.8412
Emission costs	0.26241	Natural gas purchasing costs	36.2514

Table 4 presents the components of 9-bus test system costs for different planning years. The cost of electricity purchased from the upward network took on a value 53.007 MMUs that it was about 146.22% of natural purchasing costs. The maximum and minimum installation and operation costs of the facilities were the CHP costs and boiler and TES costs, respectively. The main part of 9-bus system installation costs were CHP, electric network and DHN installation costs, respectively.

Table 4. The components of 9-bus test system costs for different planning years.

	Year					Total
Costs	1	2	3	4	5	
CHP operation costs (MMUs)	2.96125	2.78985	3.13458	3.32517	3.36214	15.57299
Energy loss costs (MMUs)	0.15214	0.16325	0.15261	0.14125	0.14798	0.75723
Electricity purchased from the upward network costs (MMUs)	6.2325	8.2412	10.1987	13.1632	15.1714	53.007
Feeder and EES operation costs (MMUs)	0.69214	0.78215	0.83621	0.97841	0.96215	4.25106
DRP costs (MMUs)	0.8127	0.8314	0.8624	0.8514	0.8782	4.2361
Boiler and TES investment and operation costs (MMUs)	0.3215	0.3612	0.4521	0.4214	0.5142	2.0704
DHN investment and operation costs (MMUs)	5.9562	0.5921	0.6213	0.6318	0.7123	8.5137
AIMGs electricity transaction Benefits (MMUs)	0.5236	0.6598	0.7521	0.8614	0.9512	3.7481

Fig. 10. (a) and (b) show the stacked column of the estimated optimal hourly heating and electricity dispatch for the final planning horizon of the 9-bus system, respectively. The CHPs were at full load when they were committed and the main part of the heating load was supplied by the boilers.

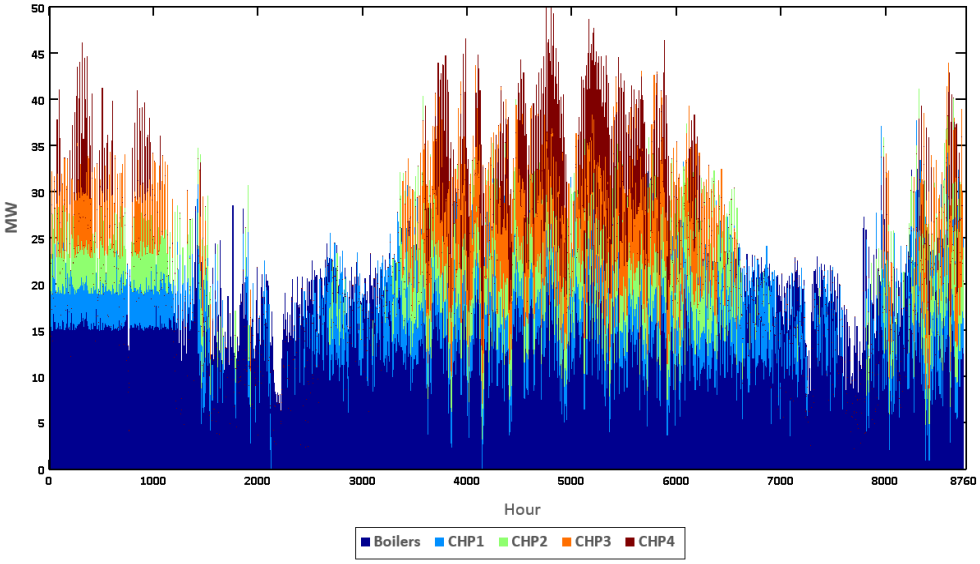

(a)

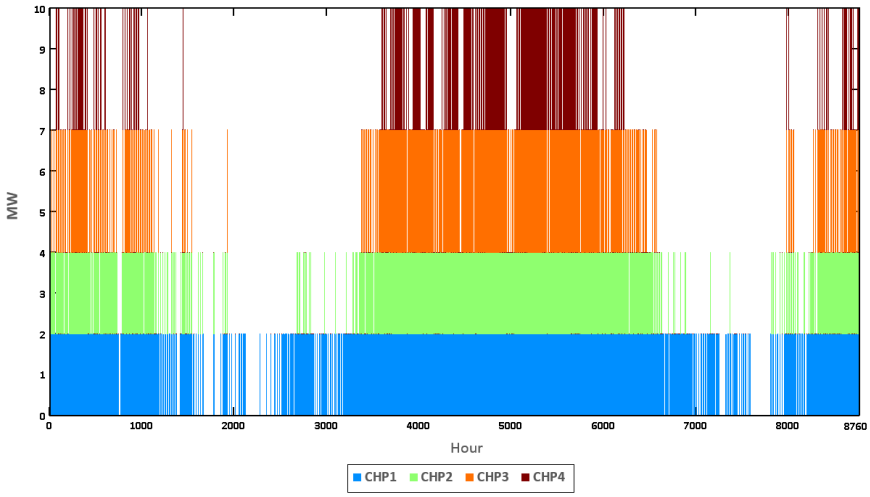

(b)

Fig. 10. (a) The stacked column of the estimated optimal heating dispatch for the final planning horizon of the 9-bus system. (b) The stacked column of the estimated optimal electricity dispatch for the final planning horizon of the 9-bus system.

Fig. 11 (a) and (b) show the estimated values of the PVAs and SWTs electricity generation for the final planning horizon of the 9-bus system, respectively. The maximum value of PVAs electricity generation was about 5.96 MW. Further, the maximum value of SWTs electricity generation was about 50 kW.

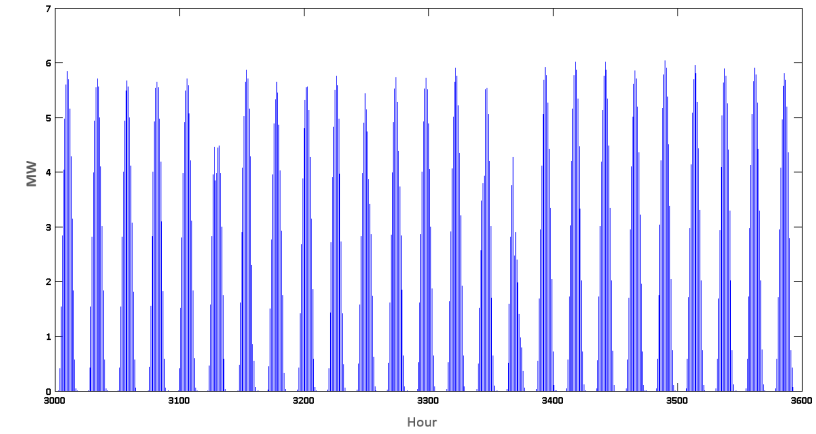

(a)

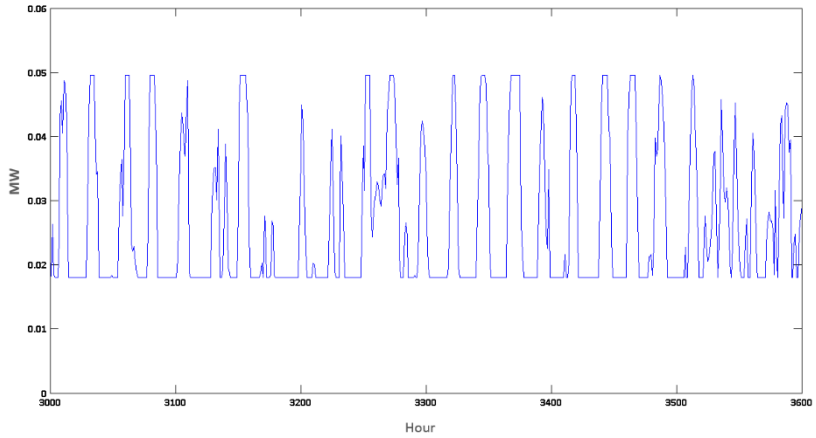

(b)

Fig. 11. (a) The stacked column of the estimated PVAs electricity generation for the final planning horizon of the 9-bus system. (b) The stacked column of the estimated SWTs electricity generation for the final planning horizon of the 9-bus system.

Fig. 12 depicts the estimated values of per-unit DLC, DERs electricity generation and electricity purchased from the upward network for the final planning horizon of the 9-bus system. The maximum value of DERs electricity generation was about 0.67 PU. Further, the maximum value of DLC was about 0.286 PU. The DCNEP utilized the DLC procedure to minimize the operational costs and involuntary load shedding in contingent conditions of the system.

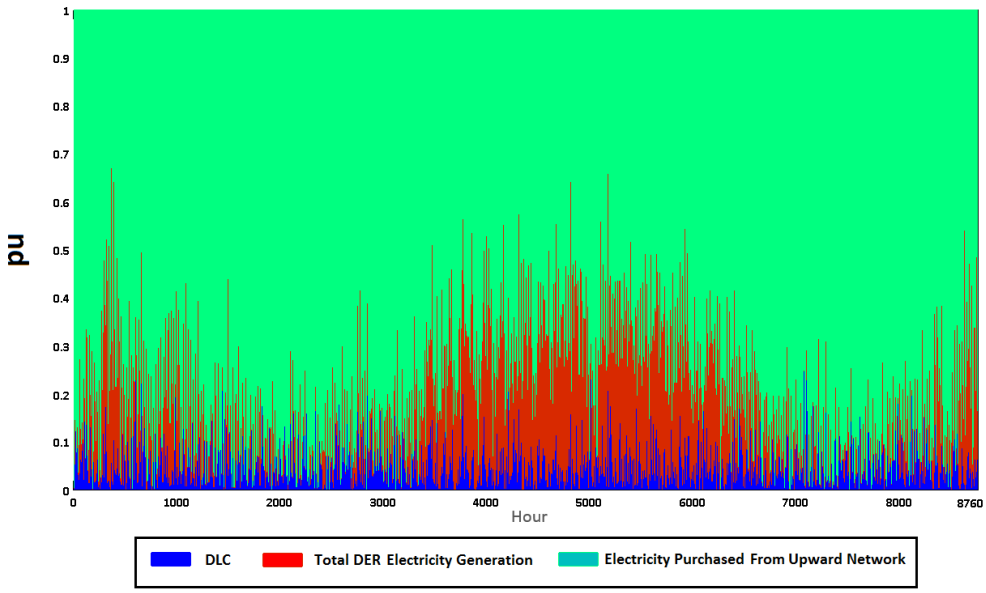

Fig. 12. The estimated values of per-unit DLC, DERs electricity generation and electricity purchased from the upward network for the final planning horizon of the 9-bus system.

Fig. 13 presents the estimated heating dispatch for different DHN of the 9-bus system and the final planning horizon. The maximum capacity of DHN was utilized to supply the heating load of the system.

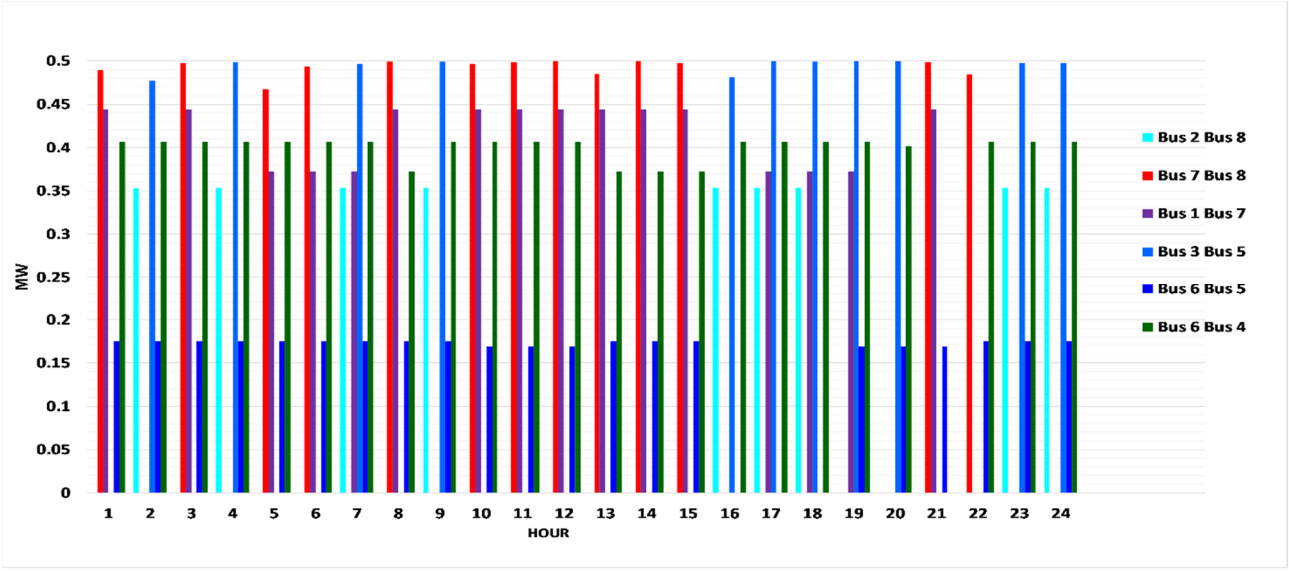

Fig. 13. The estimated heating dispatch for different DHN of the 9-bus system and the final planning horizon.

To assess the proposed optimization algorithm for the 9-bus test system, the whole state-space of the DCNEP was searched based on the fact that the search space of the 9-bus system was not very large. The full search method saved all of the feasible solutions and evaluated them to find the absolute optimum solution. The algorithm codes were developed in MATLAB and the simulation was carried out on a PC (Intel Core i7, quad-core, 2.93 GHz, 8 GB RAM). The simulation time for the proposed IAGA algorithm and the full search method for the 9-bus tests system were about 2861 seconds and 23746 seconds, respectively.

Table 5 depicts the results of the optimal outputs of DCNEP for the 9-bus test system that was determined by the full search method. Further, Table 6 presents the optimal operational costs of the 9-bus test system for different planning years that was calculated by the full search method. By comparing the corresponding value of presented tables, it can be concluded that the proposed IAGA-based DCNEP found the absolute optimal solution of state-space.

Table 5. The solution of the full search method for DCNEP of the 9-bus test system.

Costs (MMUs)			
Feeders installation costs	4.1514	Transformers and feeders operation costs	4.215
Transformer and ESS installation costs	9.2102	CHP installation and operation costs	26.8213
ENSCs	0.39265	Energy loss costs	0.75723
PVA installation and maintenance costs	4.2315	Wind turbine installation and maintenance costs	3.8412
Emission costs	0.26241	Natural gas purchasing costs	36.2514

Table 6. The full search solution for optimal operational costs of the 9-bus test system for different planning years.

	Year					Total
Costs	1	2	3	4	5	
CHP operation costs (MMUs)	2.96125	2.78985	3.13458	3.32517	3.36214	15.57299
Energy loss costs (MMUs)	0.15214	0.16325	0.15261	0.14125	0.14798	0.75723
Electricity purchased from the upward network costs (MMUs)	6.2325	8.2412	10.1987	13.1632	15.1714	53.007
Feeder and EES operation costs (MMUs)	0.69214	0.78215	0.83621	0.97841	0.96215	4.25106
DRP costs (MMUs)	0.8127	0.8314	0.8624	0.8514	0.8782	4.2361
Boiler and TES investment and operation costs (MMUs)	0.3215	0.3612	0.4521	0.4214	0.5142	2.0704
DHN investment and operation costs (MMUs)	5.9562	0.5921	0.6213	0.6318	0.7123	8.5137
AIMGs electricity transaction benefits (MMUs)	0.5236	0.6598	0.7521	0.8614	0.9512	3.7481

B. The 33-bus test system

The 33-bus test system data is presented at [50]. Fig. 14 shows the 33-bus system topology. Fig. 15 shows the hourly thermal and electrical load of the 33-bus system for the final year of the planning horizon. Fig. 16 shows the forecasted market price for the base year. The 33-bus system has a different pattern of electrical and heating load with respect to the 9-bus test system electrical and heating loads and the 33-bus system heating load is more than its electrical load.

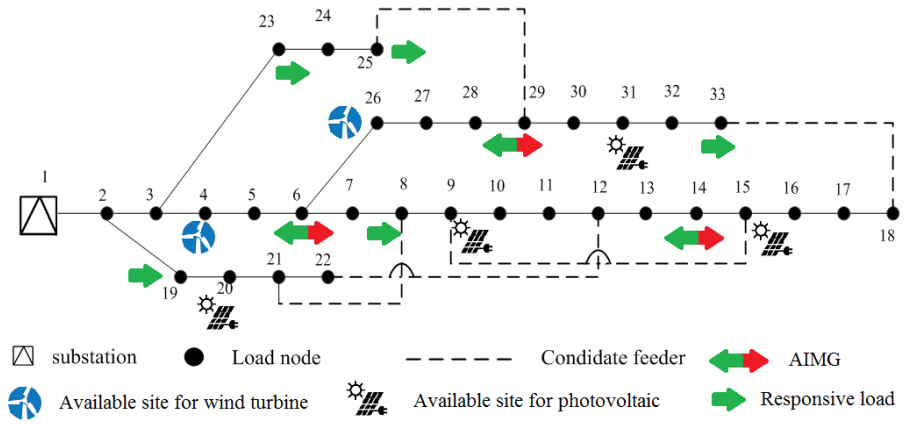

Fig. 14. The 33-bus test system.

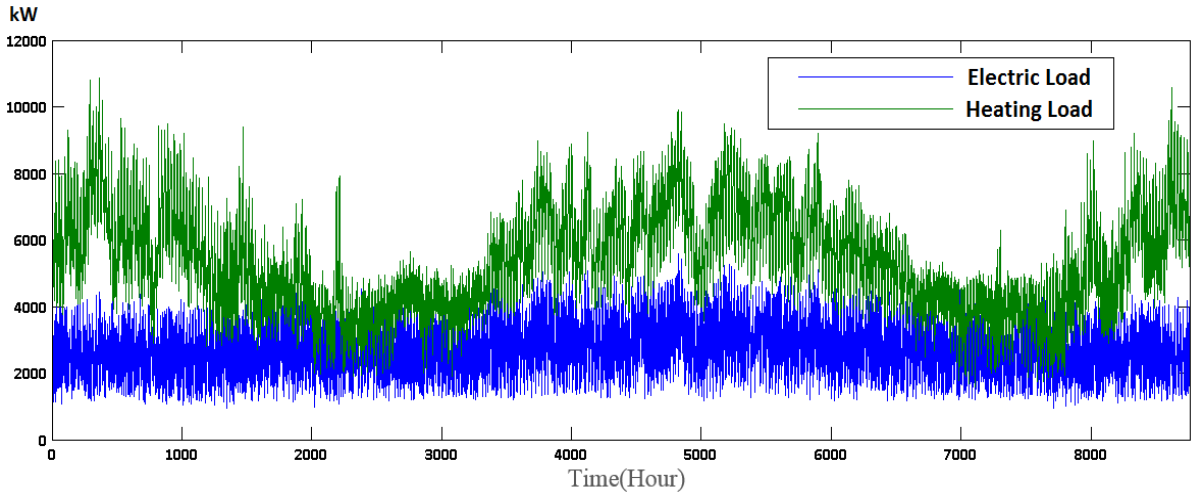

Fig.15. Hourly thermal and electrical load of the 33-bus system for the final year of the planning horizon.

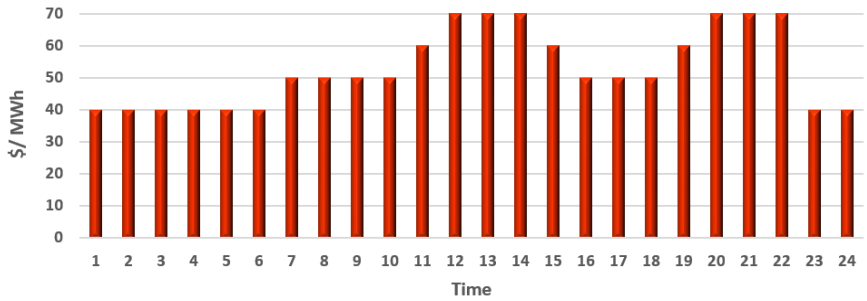

Fig. 16. The base electricity price of the upward network of the 33-bus test system.

Table A5 of the appendix shows the DCNEP parameters for the 33-bus test system. Table A6 of the appendix presents the characteristics of CHPs for the 33-bus test system. Table 7 presents the feasible and optimum AIMGs' electricity transaction cases for the electric load peak condition. The optimal value of electricity transaction is shown in green.

Table 7. The feasible and optimum AIMGs' electricity transaction cases for the 33-bus system electric load peak condition.

From	To							
Bus 6	Bus 19 (55.32) kW	Bus 20 (49.28) kW	Bus 21 (43.17) kW	Bus 22 (38.96) kW	Bus 23 (32.45) kW	Bus 24 (27.69) kW	Bus 25 (25.32) kW	--
Bus 14	Bus 19 (58.93) kW	Bus 20 (53.21) kW	Bus 21 (47.14) kW	Bus 22 (42.89) kW	Bus 23 x	Bus 24 x	Bus 25 x	Bus 26 (32.98) kW
Bus 14	Bus 27 (28.54) kW	Bus 28 (25.14) kW	Bus 29 (19.89) kW	Bus 30 (12.62) kW	Bus 31 (7.59) kW	Bus 32 x	Bus 33 x	--
Bus 29	Bus 2 (62.78) kW	Bus 3 (59.12) kW	Bus 4 (51.62) kW	Bus 5 (47.63) kW	Bus 6 (42.87) kW	Bus 7 (36.41) kW	Bus 8 (31.14) kW	Bus 9 (27.15) kW
Bus 29	Bus 10 (22.32) kW	Bus 11 (17.45) kW	Bus 12 (12.89) kW	Bus 13 (7.65) kW	Bus 14 x	Bus 15 x	Bus 16 x	Bus 17 x
Bus 29	Bus 18 x	Bus 19 (38.96) kW	Bus 20 (31.72) kW	Bus 21 (25.69) kW	Bus 22 (19.45) kW	Bus 23 (14.32) kW	Bus 24 (7.39) kW	Bus 25 x

The optimal electric system and DHN topologies of the 33-bus test system for the different years of expansion planning horizon are depicted in Fig. 17.

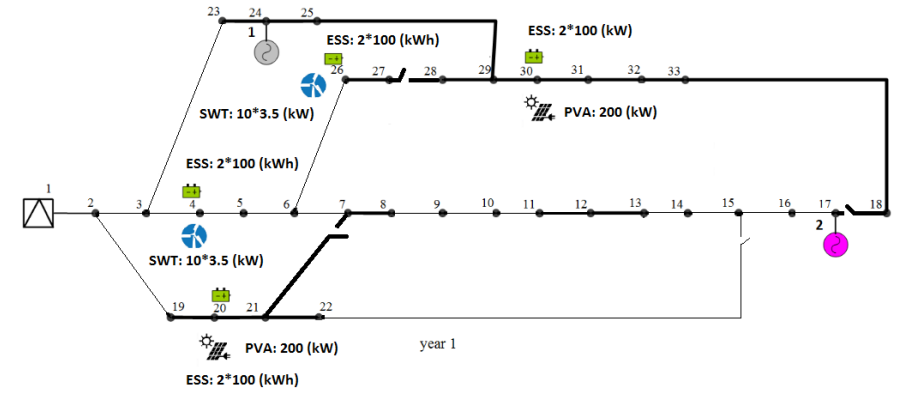

(a)

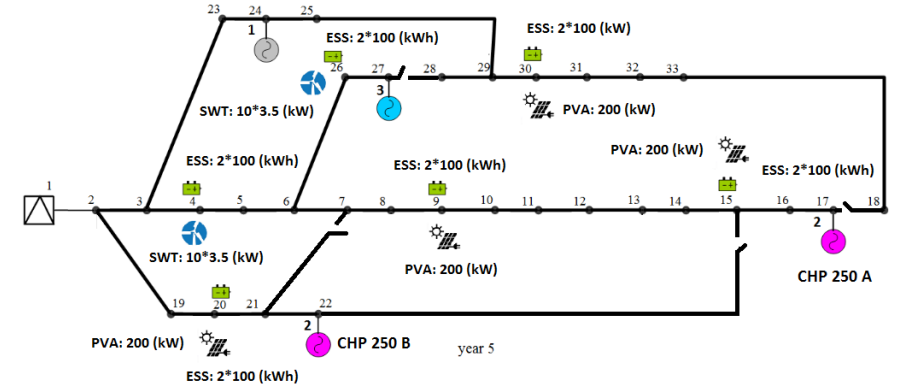

(b)

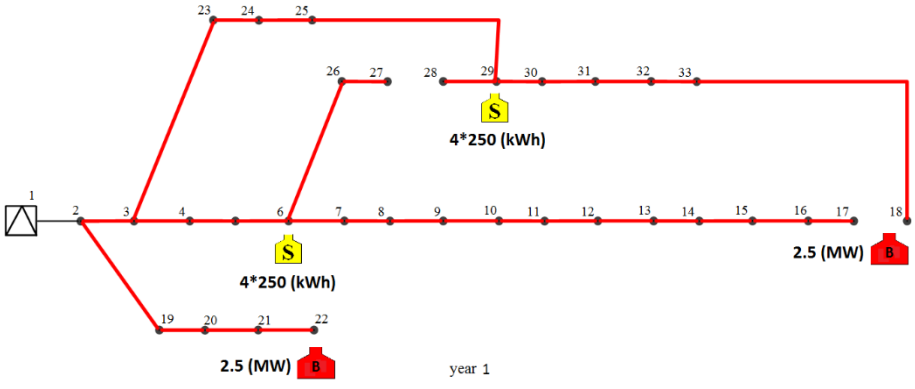

(c)

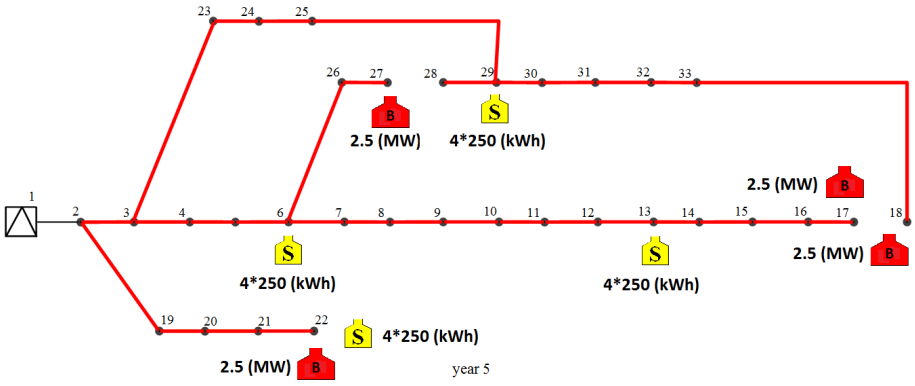

(d)

Fig. 17. (a) The optimal electrical system topology of the 33-bus test system for the 1st year of the expansion planning horizon, (b) The optimal electrical system topology of the 33-bus test system for the 5th year of the expansion planning horizon. (c) The optimal DHN topology of the 33-bus test system for the 1st year of the expansion planning horizon, (d) The optimal DHN topology of the 33-bus test system for the 5th year of the expansion planning horizon.

The DCNEP installed the maximum available capacity of SWTs in the first year of planning. However, the DCNEP installed more PVAs, ESSs, CHPs, TESs and boilers for the other years of planning. The proposed algorithm installed switching devices to perform the third stage optimization procedure in contingent conditions and restore the system's electrical loads. Table 8 depicts the optimal outputs of DCNEP for the 33-bus test system.

Table 8. The optimal outputs of DCNEP for the 33-bus test system.

	Year					Total
Costs	1	2	3	4	5	
CHP operation costs (MMUs)	0.31251	0.32987	0.33415	0.34512	0.35984	1.68149
Energy loss costs (MMUs)	0.01621	0.01715	0.01421	0.01485	0.01325	0.07567
Energy purchased from the upward network costs (MMUs)	0.53315	0.74281	0.92145	1.01874	1.51914	4.73529
Feeder and EES operation costs (MMUs)	1.62321	1.85271	1.94215	1.78151	1.96214	9.16172
DRP costs (MMUs)	0.07512	0.09874	0.06951	0.07415	0.06841	0.38593
Boiler and TES investment and operation costs (MMUs)	0.04612	0.05125	0.05214	0.06521	0.07247	0.28719
DHN investment and operation costs (MMUs)	9.1217	0.9215	0.9142	0.9214	0.9217	12.8005
AIMGs electricity transaction benefits (MMUs)	0.03652	0.07524	0.08621	0.09741	0.12152	0.4169

Table 9 presents the optimal operational costs of the 33-bus test system for different planning years.

Table 9. The optimal operational costs of the 33-bus test system for different planning years.

Costs (MMUs)			
Feeders installation costs	17.4512	Transformers and feeders operation costs	19.7841
Transformer and ESS installation costs	38.6512	CHP installation and operation costs	3.1521
ENSCs	0.42361	Energy loss costs	0.07567
PVA installation and maintenance costs	0.5124	Wind turbine installation and maintenance costs	1.9815
Emission costs	0.095214	Natural gas purchasing costs	26.96251

The DCNEP installed the maximum capacity of DHN facilities in the first year of planning and it installed more TESs and boilers for the next years. The cost of electricity purchased from the upward network took on a value 4.73529 MMUs that it was about 15.81% of natural purchasing costs. The maximum and minimum installation and operation costs of the facilities were the transformer and ESS installation costs and boiler and TESs installation costs, respectively.

Fig. 18. (a) and (b) show the stacked column of the estimated optimal hourly heating and electricity dispatch for the final planning horizon of the 33-bus system, respectively. The 330 kW CHP was fully committed and other CHPs tracked the load. The CHPs were fully loaded when they were on.

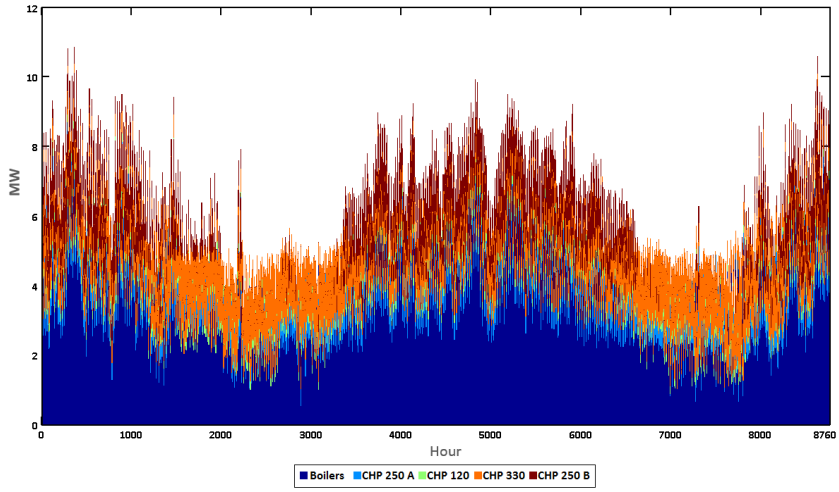

(a)

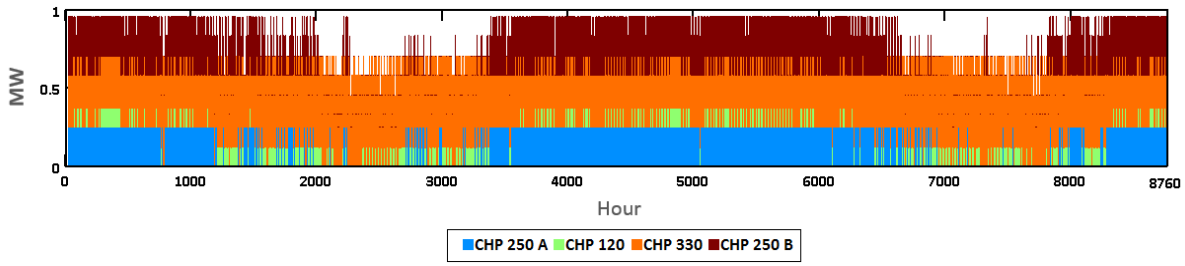

(b)

Fig. 18. (a) The stacked column of the estimated optimal heating dispatch for the final planning horizon of the 33-bus system. (b) The stacked column of the estimated optimal electricity dispatch for the final planning horizon of the 33-bus system.

Fig. 19 (a) and (b) show the estimated values of the SWTs and PVAs electricity generation for the final planning horizon of the 33-bus system, respectively. The maximum value of PVAs electricity generation was about 0.789 MW. Further, the maximum value of SWTs electricity generation was about 70 kW.

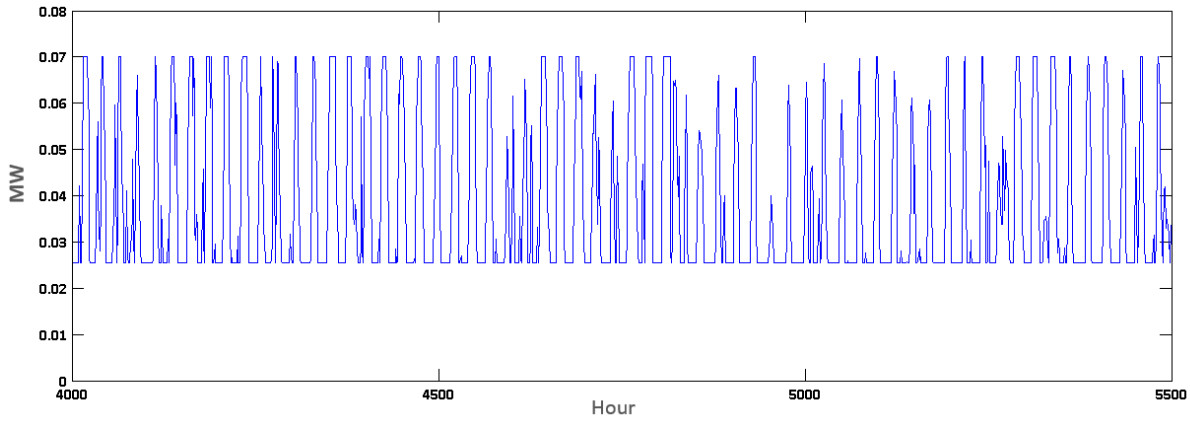

(a)

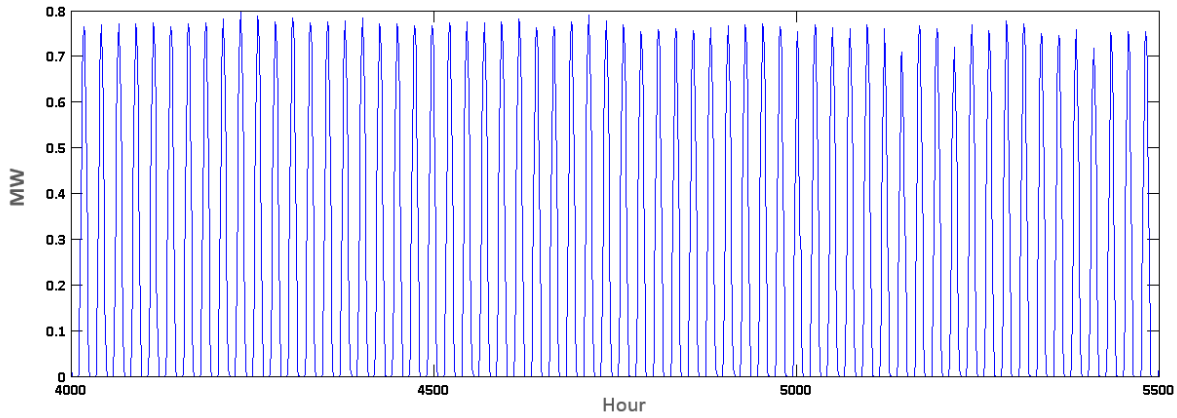

(b)

Fig. 19. (a) The stacked column of the estimated SWTs electricity generation for the final planning horizon of the 33-bus system. (b) The stacked column of the estimated PVAs electricity generation for the final planning horizon of the 33-bus system.

Fig. 20 depicts the per-unit values of DLC, DERs electricity generation and electricity purchased from the upward network for the final planning horizon of the 33-bus system. The maximum value of DERs electricity generation was about 0.681 PU. The maximum value of DLC was about 0.351 PU.

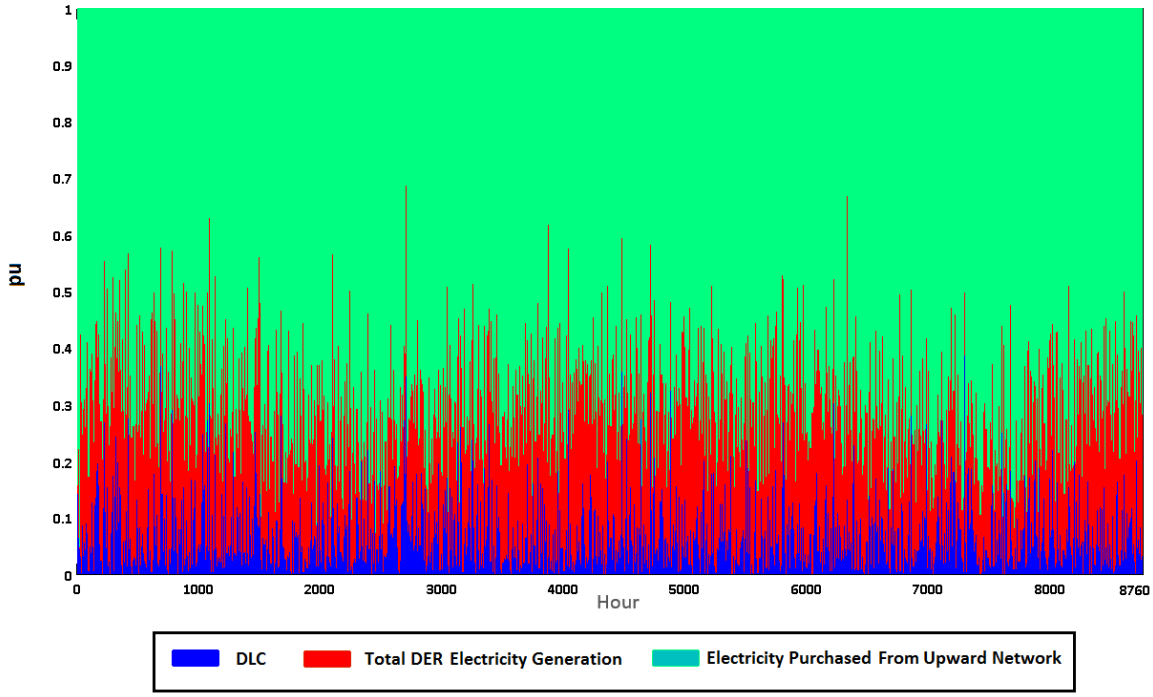

Fig. 20. The per-unit values of DLC, DERs electricity generation and electricity purchased from the upward network for the final planning horizon of the 33-bus system.

Fig. 21 (a) and (b) show the estimated values of the TESs and ESSs optimal charge and discharge for the peak periods of electrical and heating systems and the final planning horizon of the 33-bus system, respectively. The DCNEP utilized TESs and ESSs to minimize the involuntary load shedding in contingent conditions of the system. Further, the energy storage facilities were utilized to increase the transfer capability of the electric network of the EDC and reduce the operational costs.

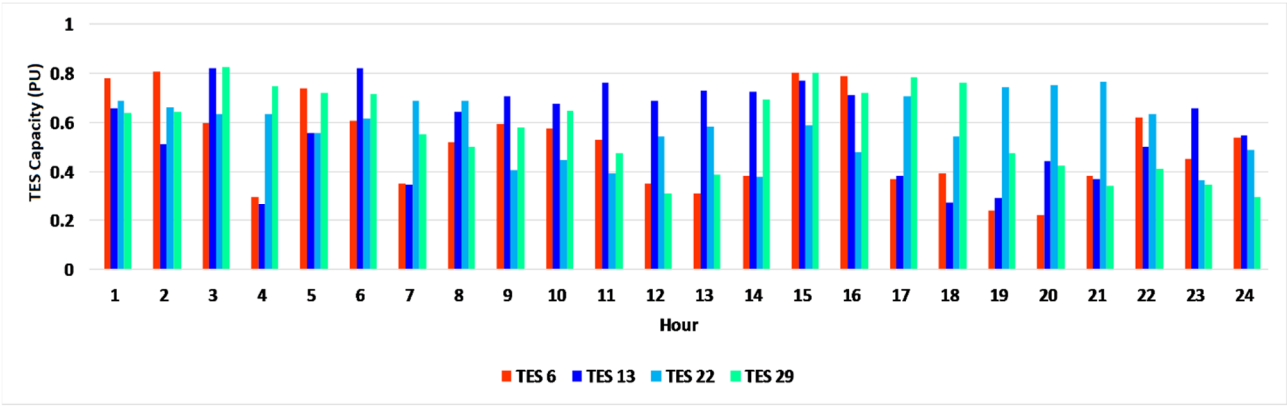

(a)

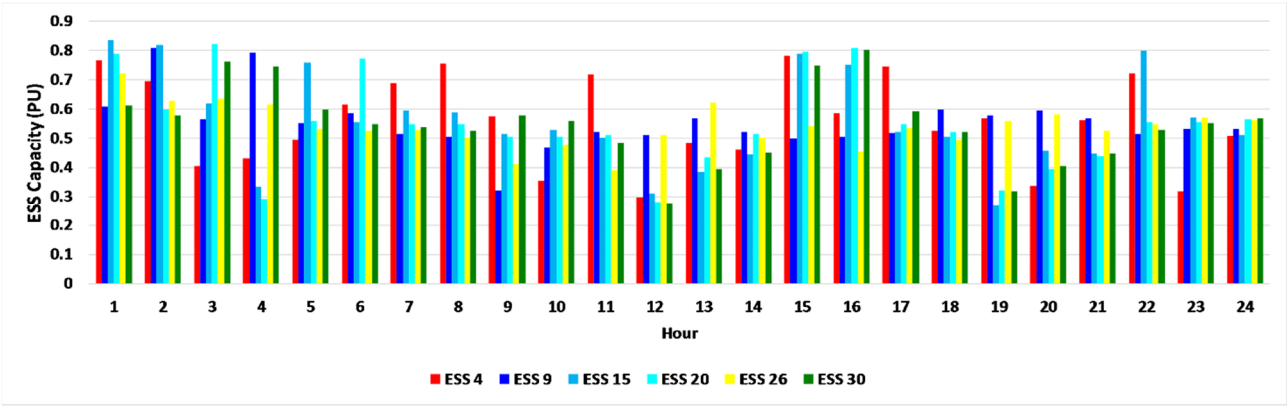

(b)

Fig. 21 (a) The estimated values of the TESs optimal charge and discharge for the peak periods of electrical and heating systems and the final planning horizon of the 33-bus system. (b) The estimated values of the EESs optimal charge and discharge for the peak periods of electrical and heating systems and the final planning horizon of the 33-bus system.

C. 123 bus system

The 123-bus test system data is presented at [51] and its topology is shown in Fig. 22. Fig. 23 depicts the estimated hourly electrical and heating loads in the final year of the planning horizon. The DCNEP parameters for the 123-bus test system are the same as their corresponding values of the 33-bus test system.

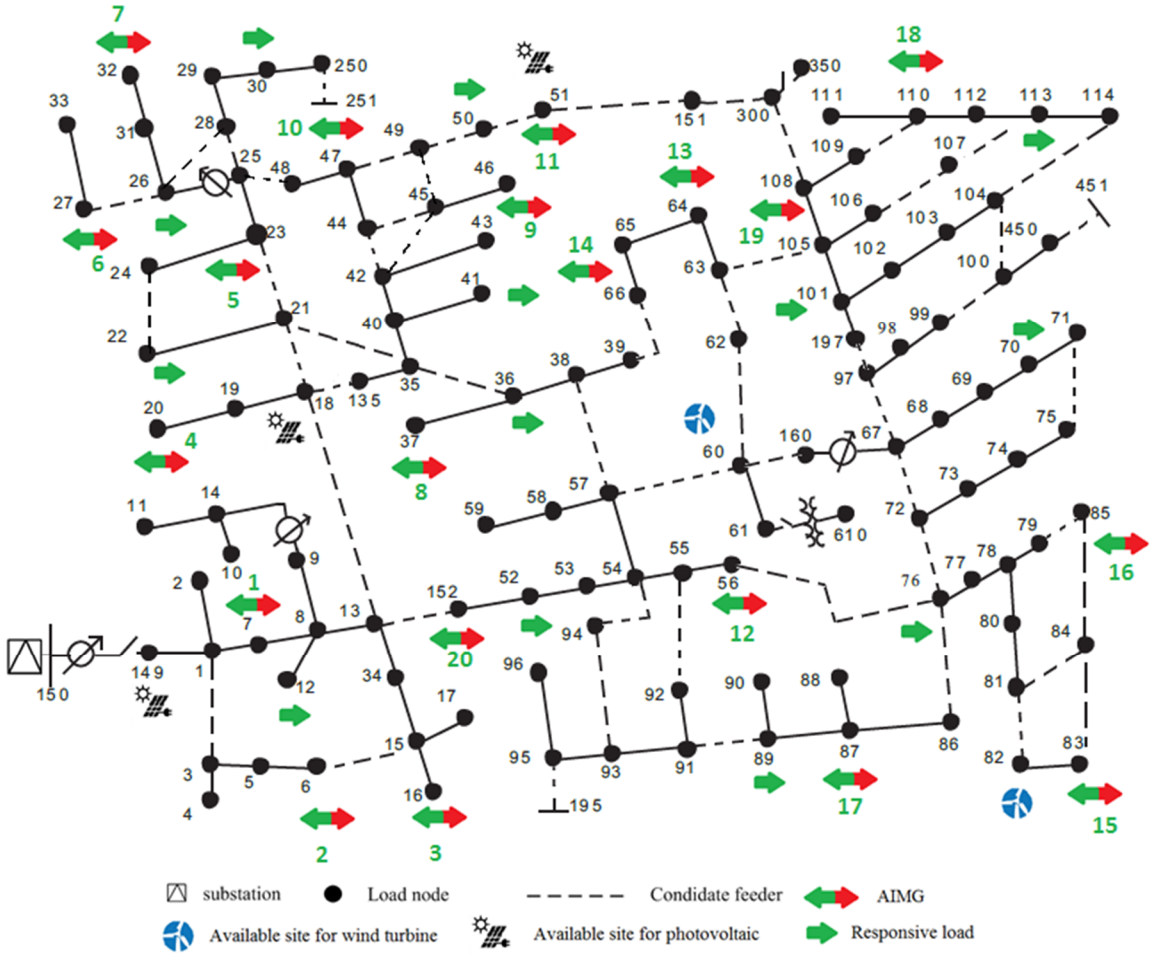

Fig.22. The 123-bus test system.

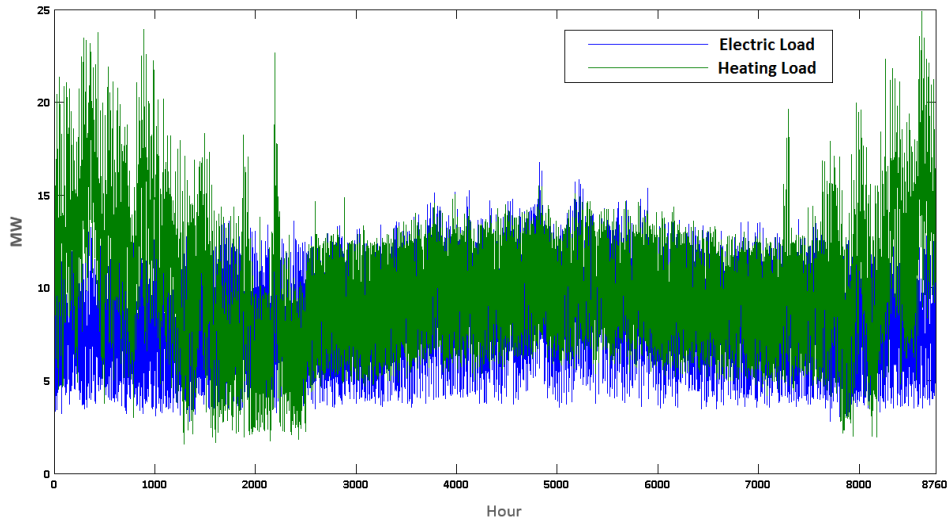

Fig.23. The hourly heating and electrical loads of the 123-bus test system for the final year.

The optimal electric system and DHN topologies of the 123-bus test system for the different years of expansion planning horizon are depicted in Fig. 24.

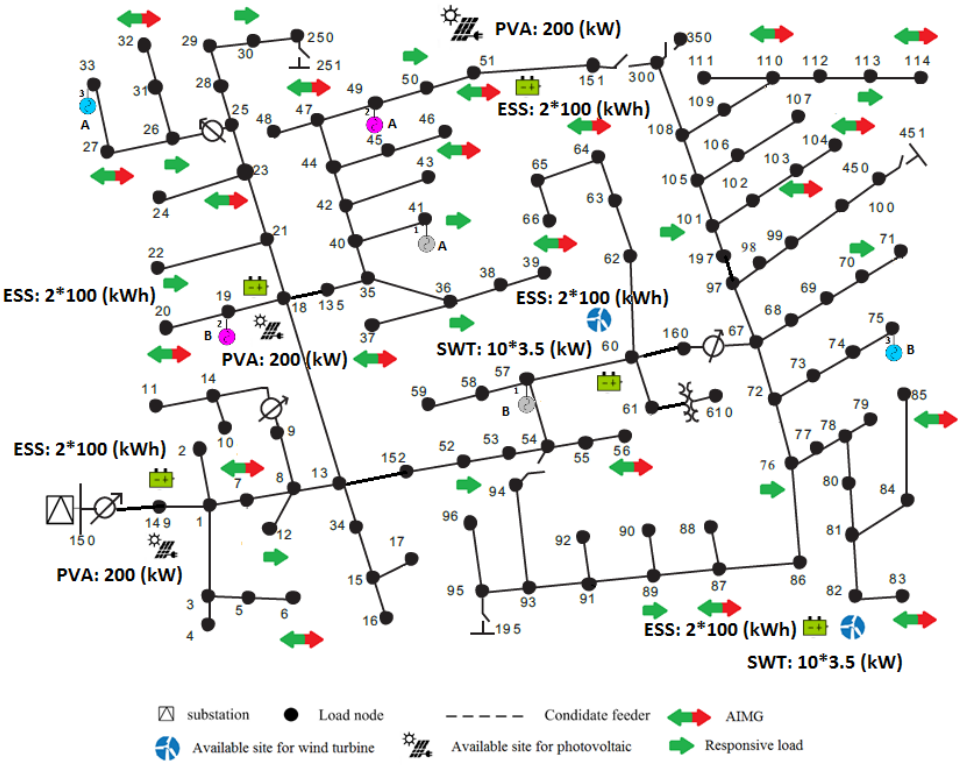

(a)

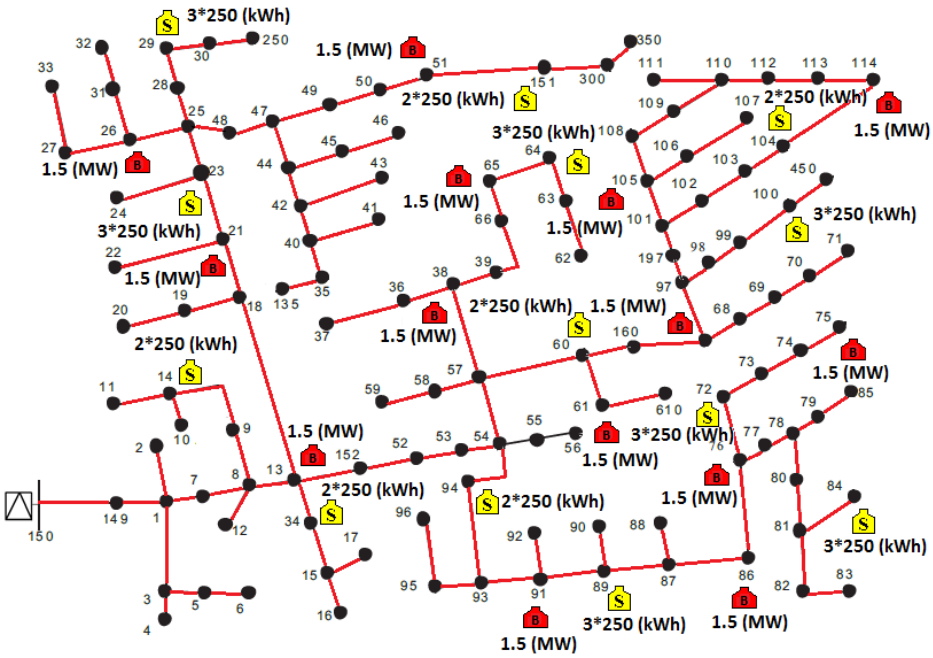

(b)

Fig. 24. (a) The optimal electrical system topology of the 123-bus test system for the 5th year of the expansion planning horizon. (b) The optimal DHN topology of the 123-bus test system for the 5th year of the expansion planning horizon.

Fig. 25 presents the feasible and optimum AIMGs' electricity transaction cases for the electric load peak condition of the fifth year of the planning year. The total number of the explored feasible and optimum AIMGs' electricity transaction cases was 53432233 and the total number of available alternatives for AIMGs' transactions was 614163600 for the overall of the planning years. Thus, the feasible and optimum AIMGs' electricity transaction was about 8.7% of the total number of transactions.

Fig. 26. (a) and (b) show the stacked column of the estimated optimal hourly heating and electricity dispatch for the final planning horizon of the 123-bus system, respectively. The 330 kW CHPs were committed for supplying of the based load and the boiler tracked the heating load. The 120 kW CHP facilities supplied the peak load of the system.

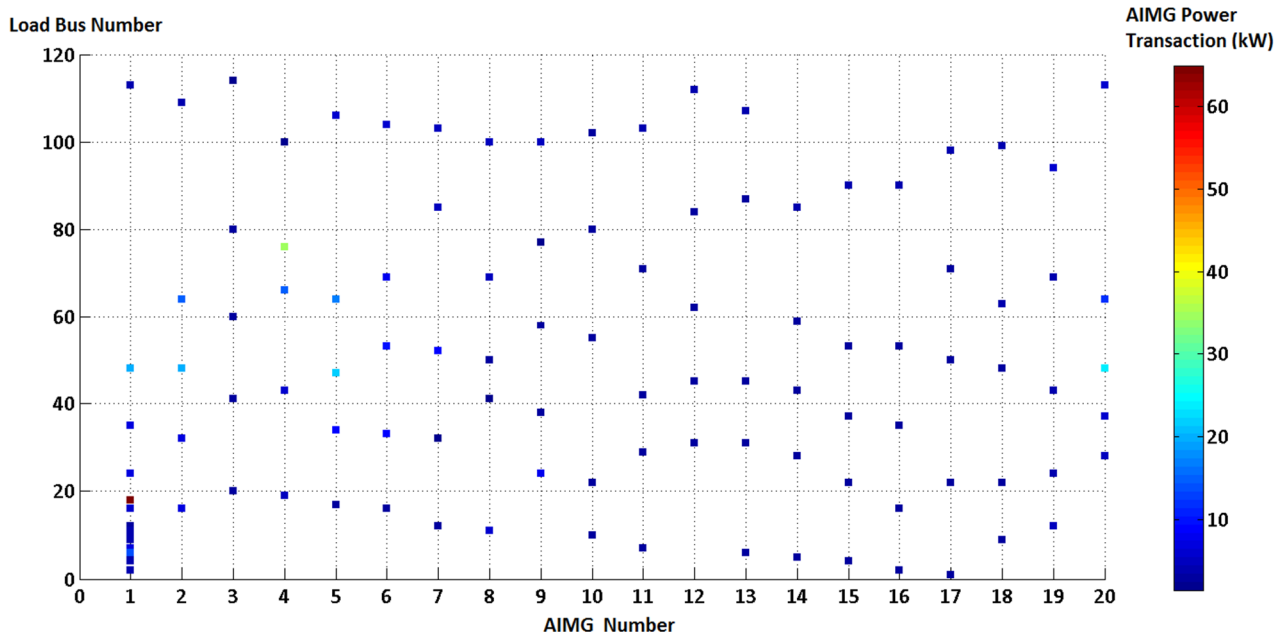

Fig.25. The feasible and optimum AIMGs' electricity transaction cases for the electric load peak condition of the 123-bus test system.

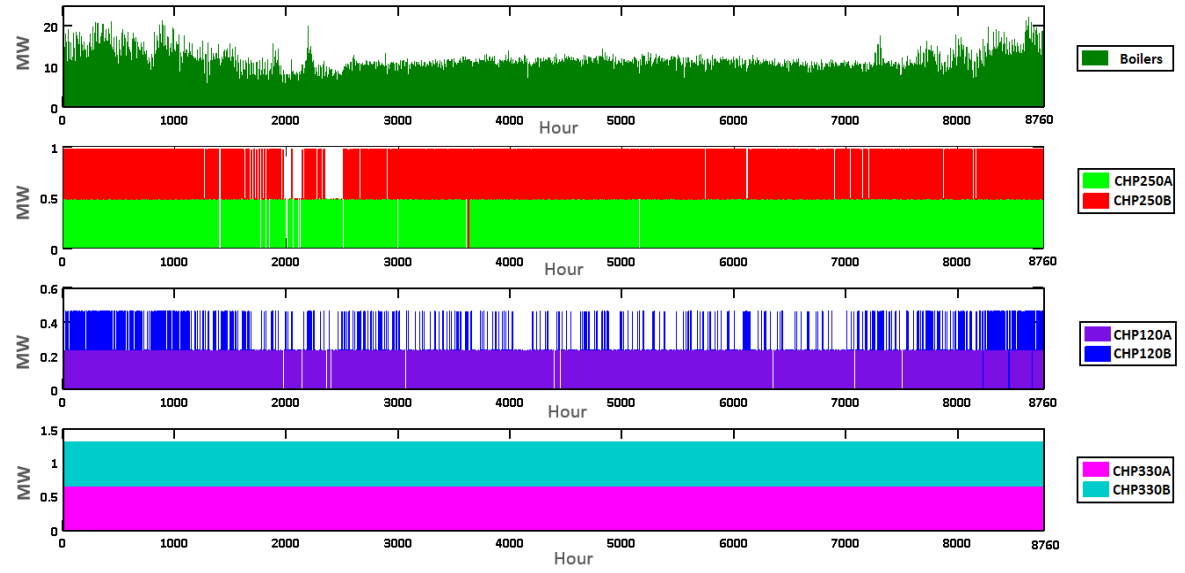

(a)

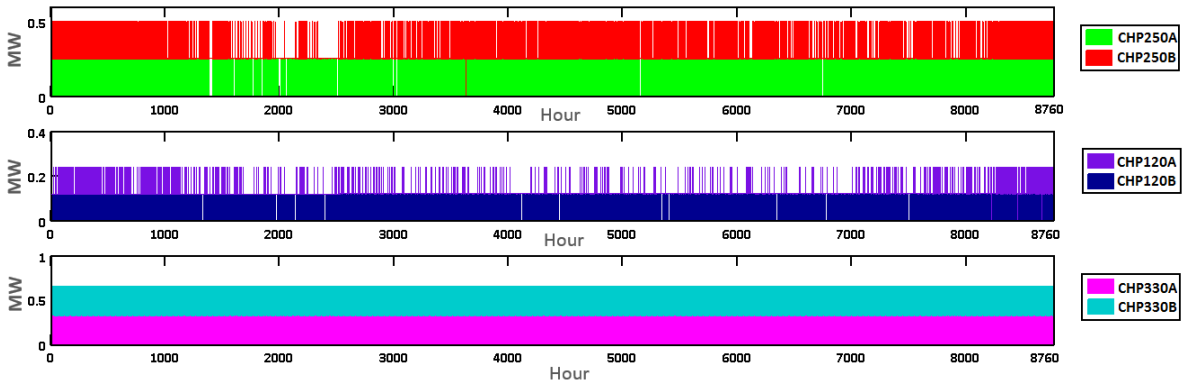

(b)

Fig. 26. (a) The stacked column of the estimated optimal heating dispatch for the final planning horizon of the 123-bus system. (b) The stacked column of the estimated optimal electricity dispatch for the final planning horizon of the 123-bus system.

Fig. 27 (a) and (b) show the estimated values of the PVAs and SWTs electricity generation for the final planning horizon of the 123-bus system, respectively. The maximum value of PVAs electricity generation was about 0.53 MW.

Fig. 28 depicts the per-unit values of DLC, DERs electricity generation and electricity purchased from the upward network for the final planning horizon of the 123-bus system. The maximum value of DERs electricity generation was about 0.473 PU.

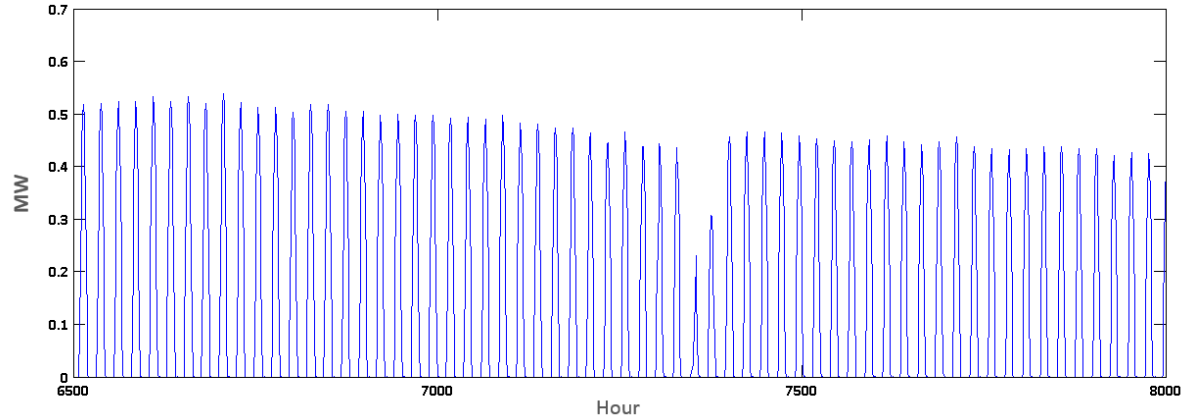

(a)

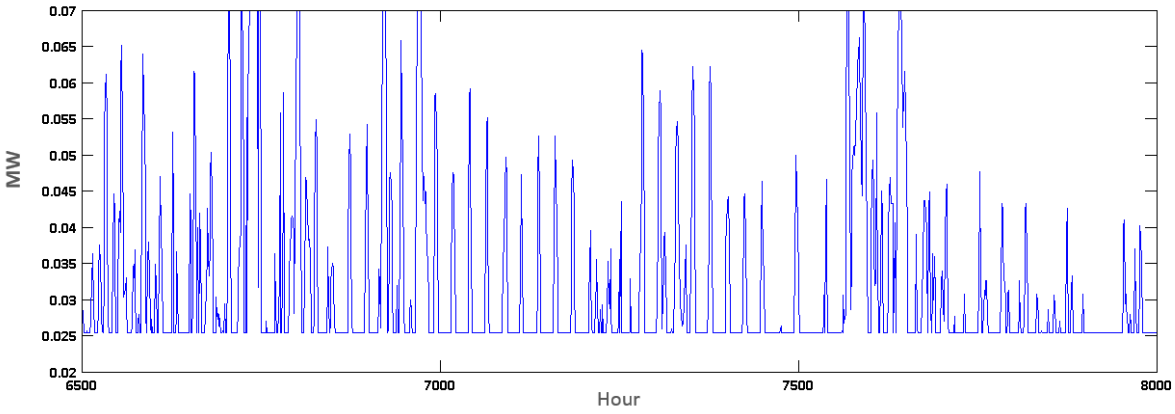

(b)

Fig. 27. (a) The PVAs electricity generation for the final planning horizon of the 123-bus system. (b) The SWTs electricity generation for the final planning horizon of the 123-bus system.

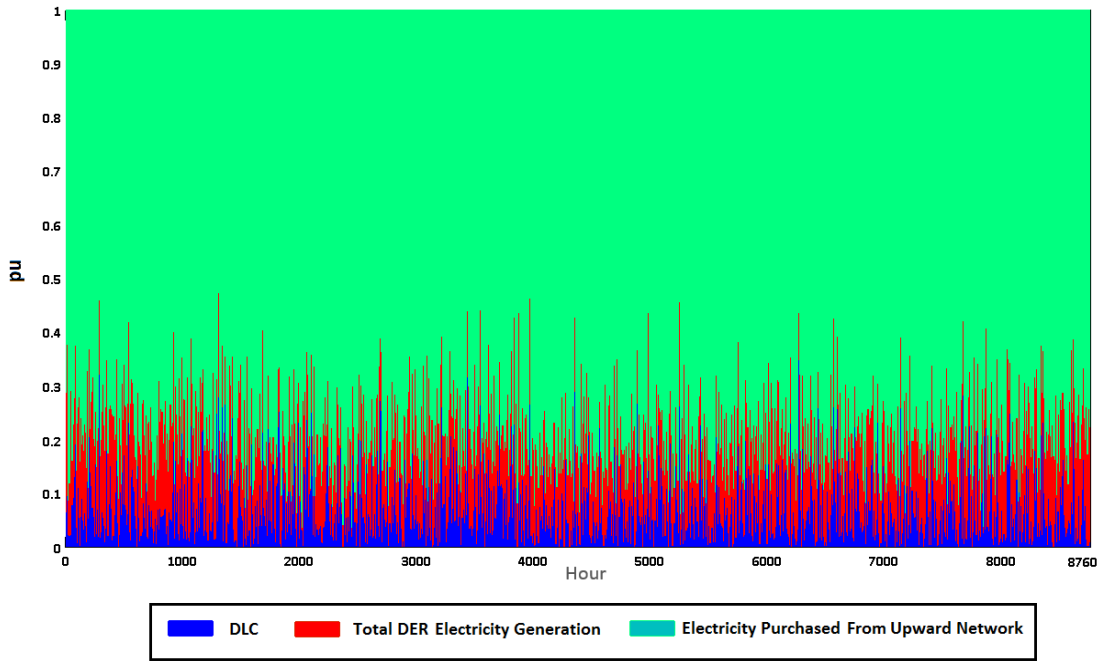

Fig. 28. The per-unit values of DLC, DERs electricity generation and electricity purchased from the upward network for the final planning horizon of the 123-bus system.

Table 10 depicts the optimal outputs of DCNEP for the 123-bus test system. The cost of electricity purchased from the upward network took on a value 11.9562 MMUs that it was about 79.77% of natural purchasing costs. The maximum and minimum installation costs of the facilities were the transformer and ESS installation costs and PVA installation costs, respectively.

Table 10. The optimal operational costs of the 123-bus test system.

Costs (MMUs)			
Feeders installation costs	70.3625	Transformers and feeders operation costs	86.2174
Transformer and ESS installation costs	157.2132	CHP installation and operation costs	5.1221
ENSCs	1.2395	Energy loss costs	0.5321
PVA installation and maintenance costs	0.5231	Wind turbine installation and maintenance costs	1.9903
Emission costs	0.1380603	Natural gas purchasing costs	14.98741
DHN investment and operation costs (MMUs)	39.3214	AIMGs electricity transaction Benefits (MMUs)	3.291
Boiler and TES investment and operation costs (MMUs)	0.965	DRP costs (MMUs)	0.9851

Further, another scenario was studied in the following case to assess the proposed DCNEP algorithm. The EDC purchased electricity from the wholesale market to supply its loads and only boilers were used to supply heating loads. This scenario is named as the second scenario of DCNEP and its results are presented in the following figures. Fig. 29 depicts the final investment, operational, emission, electricity and natural gas purchasing costs for two scenarios of the 9-bus, 33-bus and 123-bus test systems at the horizon year of planning.

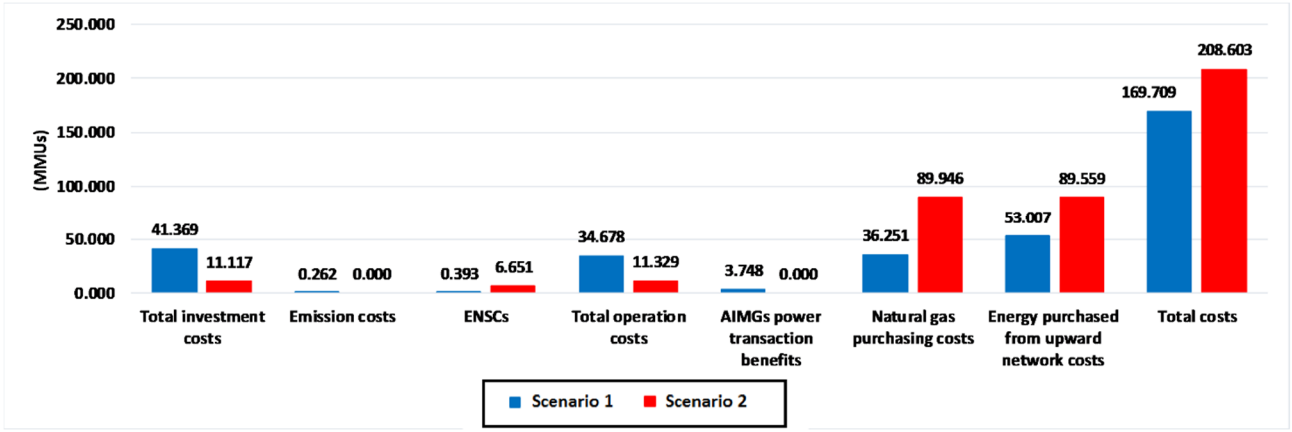

(a)

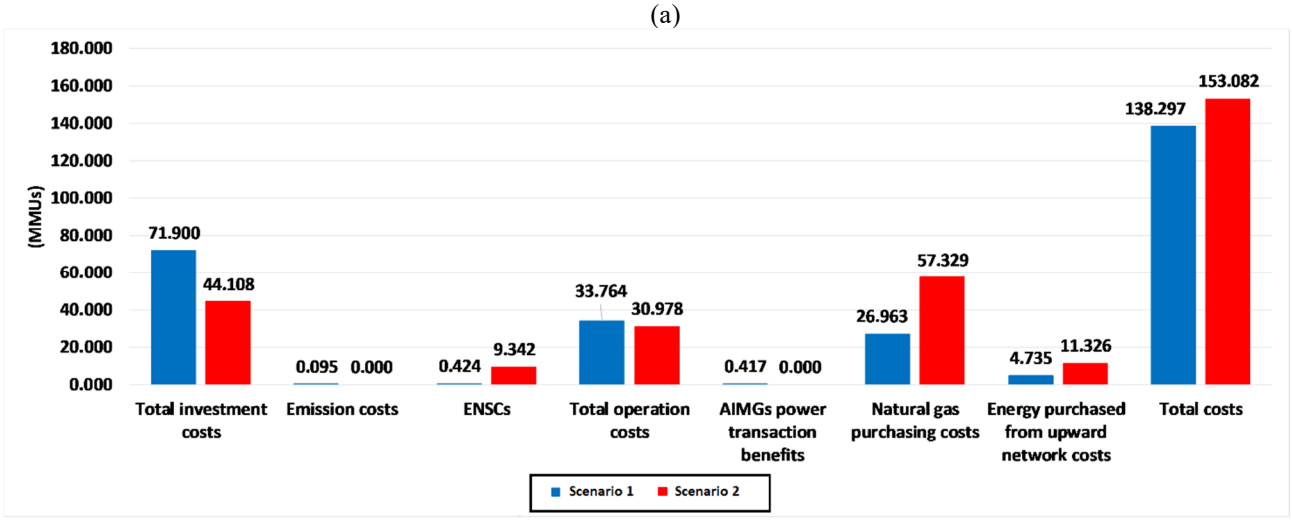

(b)

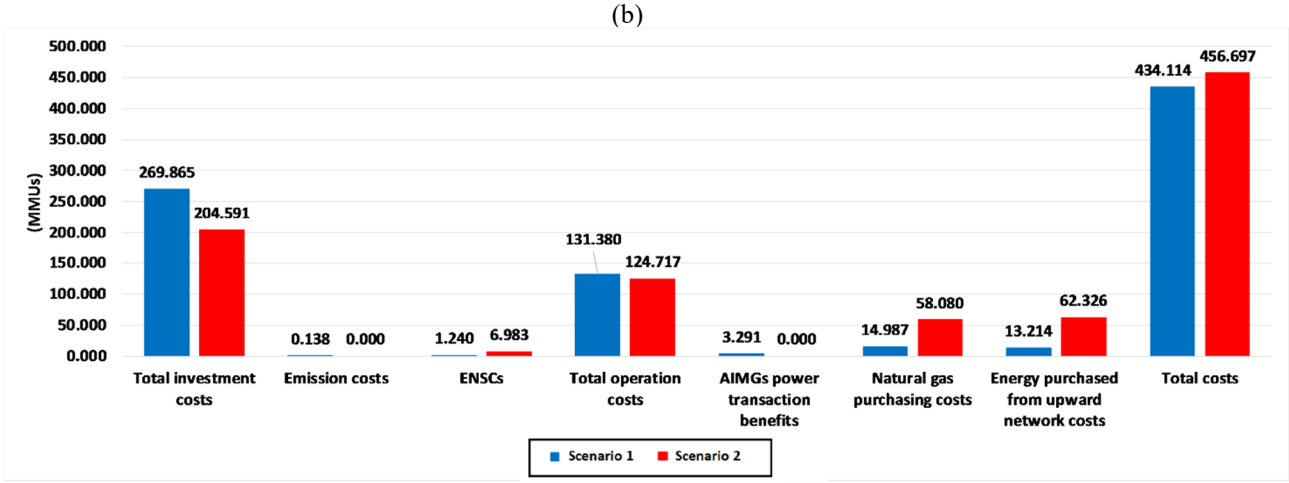

(c)

Fig. 29. The final investment, operational, emission, electricity and natural gas purchasing costs for two scenarios of (a) the 9-bus, (b) 33-bus, (c) 123-bus test systems at the horizon year of planning.

According to Fig. 29, the DCNEP reduced the aggregated total costs for the 9-bus, 33-bus and 123-bus system about 18.645%, 9.658%, and 4.849% with respect to the 2nd scenario costs, respectively. Further, the 5 years AIMGs electricity transactions benefits were about 3.7481 MMUs, 0.4169 MMUs, and 3.291 MMUs for the 9-bus, 33-bus and 123-bus test systems, respectively. It means that the EDC can gain benefit from AIMGs electricity transactions.

Table 11 shows the number of continuous and discrete variables, the number of equations, DCNEP iterations and maximum values of MWRI for final planning year for different case studies. The number of equations for the 123-bus test system was 11955854 that indicates the curse of dimensionality. The maximum CPU time required to solve the scenarios was about 14405 seconds for the 123-bus test system.

Table 11. The DCNEP algorithm computation time, the number of variables and iterations for different case studies.

Case	continuous variables	discrete variables	total equations	CPU time (sec)	Number of three-stage DCNEP iterations	Maximum value of MWRI
9-bus	352108	15840	650514	2861	2	9.6514
33-bus	1361560	29548	2332926	5982	2	7.8249
123-bus	7417838	112698	11955854	14405	3	7.9826

The proposed DCNEP algorithm successfully carried out the optimal energy resources and network expansion planning with quite acceptable results and computational burden.

5. Conclusion

This paper presented an iterative MINLP algorithm for the DCNEP problem of an EDC with multiple DERs. The proposed method considered the AIMGs' electricity transactions and minimized investment, operational and emission cost; meanwhile, maximized the EDC's system's reliability. The three-stage algorithm explored the adequacy of the EDC's system resources in the normal and contingent operational conditions; meanwhile, it considered the AIMGs electricity transactions. The evaluation of the feasibility and optimality of the AIMGs' electrical transactions imposed a very heavy computational burden on the DCNEP procedure. Three test systems were considered by different configurations, electrical and heating loads, and operational paradigms. The DCNEP reduced the aggregated total costs for the 9-bus, 33-bus and 123-bus system about 18.645%, 9.658%, and 4.849% with respect to the 2nd scenario costs, respectively. Further, the 5 years AIMGs electricity transactions benefits were about 3.7481 MMUs, 0.4169 (MMUs), and 3.291 MMUs for the 9-bus, 33-bus and 123-bus test systems, respectively. It means that the EDC can gain benefit

from AIMGs electricity transactions. The total number of the explored feasible and optimum AIMGs' electricity transaction cases of the 123-bus test system was 53432233. Further, the total number of available alternatives for AIMGs' transactions was 614163600 for overall of the planning years. The proposed three-stage optimization algorithm successfully carried out the optimal energy resources and network expansion planning with quite acceptable results and computational burden. In conclusion, the adoption of the proposed DCNEP includes AIMGs electricity transactions allows increasing significantly the EDC benefits and reliability. The authors are investigating the use of other heuristic optimization method to speed up the calculation of the DCNEP procedure.

6. Acknowledgment

J.P.S. Catalão acknowledges the support by FEDER funds through COMPETE 2020 and by Portuguese funds through FCT, under POCI-01-0145-FEDER-029803 (02/SAICT/2017).

7. Appendix

Table A1. The 9-bus system CHP installation alternatives technical characteristics and fixed and variable costs.

CHP type	Maximum output power $P_{max}(MW)$	Installation Fixed cost (MUs)	Installation variable cost (MUs/kVA)	Operation Fixed cost (MUs/kW)	Operation variable cost (MUs/kWh)
1	1	224002.2	455	0.3256	1.2153
2	2	523951	982	0.3126	1.2871
3	3	625361	1450	0.2978	1.6241

Table A2. The conductor data for the 9-bus test system.

Conductor type	Capacity (MVA)	Impedance $\frac{\Omega}{Km}$	Failure rate	Mean time to repair(hour)	Installation cost (MUs/km)
1	7.5	0.7945	0.21	3.2	30500
2	10	0.3977	0.22	3	41000
3	15	0.1986	0.21	3.2	62000

Table A3. DCNEP parameters for the 9-bus test system.

Parameter	Value
Discount rate (%)	12.5
Electric Storage efficiency (%)	0.75
Thermal Storage efficiency (%)	95
NOIS	2
NOSS	2
The heating and electrical load factor for the NOIS=2	0.7
Market price growth rate (%)	2
MWRI	10

Table A4. DERs, DHN, DRP and emission data.

	parameters
PVA	C_{Inv}^{PVA} = 1.48E+5 (MMUs/m^2 .MW), Lifetime=25(years), C_{M}^{PVA} =5.55E+01 (MMUs/MWh)
SWT	Module: 3.5(kW) @ 250 (rpm), Cut-in speed= 3(m/s), Total length=3 (m), Type: Up-wind horizontal rotor, noise: 37 dB(A) from 60 (m) with a wind speed 8 (m/s) , C_{Invest}^{SWT} =2.4E+03 (MMUs), C_{M}^{SWT} =3.7E+04 (MUs/MWh)
ESS	Max capacity=2 (MW), Modules capacity= 100 (kW), Type: Lead-acid battery, Efficiency=0.75, C_{Inv}^{ESS} =11.285E+03 (MMUs/MWh), $C_{Op}^{ESS} + C_{M}^{ESS}$ =5.55E+02 (MMUs/MWh), Lifetime=3500 (cycle number)
TES	Max capacity module =3 (MW), Modules capacity= 250 (kW), C_{Inv}^{CSS} = 6.72E+02 (MMUs/MWh) , $C_{Op}^{ESS} + C_{M}^{ESS}$ =1.8E+01 (MMUs/MWh), Lifetime=25(years)
DHN	$C_{Capacity}^{DH}$ =2.59 (MMUs/m.MW), C_{leng}^{DH} =1.221E+01 (MMUs/m), $C_{Capacity}^{DC}$ =2.59 (MMUs/m.MW), Q^{Loss} =%18 heating transmission
Boiler	Max capacity=2.5 (MW), Modules capacity= 500 (kW), C_{Invest}^{Boiler} = 1.02 (MMUs/MW) , C_{M}^{Boiler} = 4.81E+05 (MUs) , Lifetime=25(years)
Environmental emission prices	C_{CO_2} =2.59 (MMUs/ton), C_{SO_2} =3.7E+01 (MMUs/ton), C_{NO_X} =3.7E+01 (MMUs/ton)
Transmission service price	1500 (MU/kWh)
DLC price	2500 (MU/kWh)
Involuntary load Shedding price	100000 (MU/kWh)
Natural gas fuel price	0.03 (MMUs/m^3)

Table A5. DCNEP parameters for the 33-bus test system.

Parameter	Value
Discount rate (%)	12.5
Electric Storage efficiency (%)	0.80
Thermal Storage efficiency (%)	95
Number of the EDC's intermittent power generation scenarios	3500
Number of the EDC's intermittent power generation reduced scenarios	40
Number of AIMGs' power energy consumption scenarios	100
Number of AIMGs' power energy consumption reduced scenarios	10
Number of AIMGs' power transactions	From AIMGs' buses to another buses
NCSS	Number of the EDC's electric system components
The heating and electrical annual load growth	0.3
The heating and electrical load factor	0.7
Market price growth rate (%)	2
MWRI	8

Table. A6. The 33-bus system CHP installation candidates' technical characteristics and fixed and variable costs.

CHP type	Maximum output power $P_{\max}(MW)$	Installation Fixed cost (MUs)	Installation variable cost (MUs/kVA)	Operation Fixed cost (MUs/kW)	Operation variable cost (MUs/kWh)
1	120	21369	165.5	0.2688	1.0853
2	250	57894	210.3	0.2792	1.3011
3	330	65133	230.2	0.2173	1.0569

References

[1] Simone Buffa, Marco Cozzini, Matteo D'Antoni, Marco Baratieri, Roberto Fedrizzi, "5th generation district heating and cooling systems: A review of existing cases in Europe", *Renew. Sustain. Energy Revs.*, 2019, **104**, pp. 504-522.

[2] S. Chowdhury, S.P. Chowdhury and P. Crossley, "Microgrids and active distribution networks", The institution of engineering and technology, 2009.

[3] Chicco G, Mancarella P., "Distributed multi-generation: a comprehensive view", *Renew. Sustain. Energy Revs.*, 2009, **13**, pp. 535–551.

[4] Aringhieri R, Malucelli F., "Optimal operations management and network planning of a district system with a combined heat and power plant". *Annals of Operations Research,* 2003,**120**, pp.173–199.

[5] Hantao Wang, Huiming Zhang, Chenghong Gu, Furong Lid, "Optimal design and operation of CHPs and energy hub with multi objectives for a local energy system", *Energy Procedia,* 2017, **142**, pp. 1615–1621.

[6] Saeed Moradi, Reza Ghaffarpour, Ali Mohammad Ranjbar, Babak Mozaffari, "Optimal integrated sizing and planning of hubs with midsize/large CHP units considering reliability of supply", *Energy Convers. Manage.*, 2017, **148**, pp. 974–992.

[7] Abdollah Rastgou, Jamal Moshtagh," Improved harmony search algorithm for electrical distribution network expansion planning in the presence of distributed generators", *Energy,* 2018, **151**, pp. 178-202.

[8] Jose L. Mojica, Damon Petersen, Brigham Hansen, Kody M. Powell, John D. Hedengren," Optimal combined long-term facility design and short-term operational strategy for CHP capacity investments", *Energ*y, 2017, **118**, pp. 97-115.

[9] Ali Reza Abbasi, Ali Reza Seifi, "Energy expansion planning by considering electrical and thermal expansion simultaneously", *Energy Convers. Manage.* , 2014, **83**, pp. 9–18.

[10] Jin Hou, Peng Xu, Xing Lu, Zhihong Pang, Yiyi Chu, Gongsheng Huang, "Implementation of expansion planning in existing district energy system: A case study in China", *Appl. Energy*, 2018, **211**, pp. 269-281.

[11] Alessandro Franco, Michele Versace, "Optimum sizing and operational strategy of CHP plant for district heating based on the use of composite indicators", *Energy*, 2017, **124**, pp. 258-271.

[12] Axelle Delangle, Romain S. C. Lambert, Nilay Shah, Salvador Acha, Christos N. Markides, "Modelling and optimising the marginal expansion of an existing district heating network", *Energy*, 2017, **140,** pp. 209-223.

[13] Chiara Bordin, Angelo Gordini, Daniele Vigo, "An optimization approach for district heating", *European J. Oper. Res.*, 2016, **252,** pp. 296-307.

[14] Mohammad Sameti, Fariborz Haghighat, "Optimization of 4th generation distributed district heating system: Design and planning of combined heat and power", *Renew. Energy*, 2019, 1**30**, pp. 371-378.

[15] T. Mertz, S.Serra , A.Henon , J.M. Reneaume, "A MINLP optimization of the configuration and the design of a district heating network: Academic study cases", *Energy*, 2016, **117**, pp. 450-464.

[16] Bei Lia, Robin Rochea, Damien Paire, Abdellatif Miraoui, "Optimal sizing of distributed generation in gas/electricity/heat supply networks", *Energy*, 2018, **151**, pp. 675-688.

[17] Weber C, Shah N., "Optimization based design of a district energy system for an eco-town in the united kingdom", *Energy*, 2011, **36**, pp.1292–1308.

[18] Soderman J, Petterson F., "Structural and operational optimization of distributed energy systems", *Appl. Thermal Engineering*, 2006, **26**, pp. 1400–1408.

[19] Mehleri ED, Sarimveis H, Markatos NC, Papageorgiou LG, "Optimal design and operation of distributed energy systems: application to Greek residential sector", *Renew. Energy*, 2013, **51**, pp. 331–342.

[20] Bracco S, Gabriele D, and Silvia S., "Economic and environmental optimization model for the design and the operation of a combined heat and power distributed generation system in an urban area", *Energy*, 2013, 55, pp. 1014–1024.

[21] Mohammad Hadi Shaban Boloukat, Asghar Akbari Foroud, "Stochastic-based resource expansion planning for a grid-connected microgrid using interval linear programming", *Energy,* **113**, pp. 776-787, 2016.

[22] Yokoyama, Ryohei, Yasushi Hasegawa, and Koichi Ito. "A MILP decomposition approach to large scale optimization in structural design of energy supply systems." *Energy Convers. Manage.*, 2002, **43**, (6), pp. 771-790.

[23] Houman Jamshidi Monfared, Ahmad Ghasemi, Abdolah Loni, Mousa Marzband, "A hybrid price-based demand response program for the residential micro-grid", *Energy*, 2019, **185**, pp.274-285.

[24] Mousa Marzband, Fatemeh Azarinejadian, Mehdi Savaghebi, Edris Pouresmaeil, Josep M. Guerrero, Gordon Lightbody," Smart Transactive energy framework in grid-connected multiple home microgrids under independent and coalition operations", *Renew. Energy*, 2018, **126**, pp. 95-106.

[25] Hamid Reza Gholinejad, Abdolah Loni, Jafar Adabi, Mousa Marzband, "A hierarchical energy management system for multiple home energy hubs in neighborhood grids", *J. of Building Engineering,* 2020,**20** , 101028.

[26] Lazaros Gkatzikis, Iordanis Koutsopoulos, Theodoros Salonidis, "The role of aggregators in smart grid demand response markets", *IEEE J. on Selected Areas in Communications*, 2013, **31**, no. 7, 2014, **5**, no. 4, pp. 1247-1257.

[27] Nikolaos G. Paterakis, Akin Tascikaraoglu, Ozan Erdinc, Anastasios G. Bakirtzis, João P. S. Catalão, "Assessment of demand response driven load pattern elasticity using a combined approach for smart households", *IEEE Trans. Industrial Informatics,* 2016, **12**, 4, pp. 1529-1539.

[28] Fei Wang, Kangping Li, Chun Liu, Zengqiang Mi, Miadreza Shafie-khah, João P. S. Catalão, "Synchronous pattern matching principle based residential demand response baseline estimation: Mechanism analysis and approach description", *IEEE Trans. Smart Grid, 2018*, **9**, no. 6, pp. 6972-6985.

[29] Tohid Khalili, Amirreza Jafari, Mehdi Abapour, Behnam Mohammadi-Ivatloo," Optimal battery technology selection and incentive-based demand response program utilization for reliability improvement of an insular microgrid", *Energy*, 2019, **169**, pp. 92-104.

[30] F. Wang, B. Xiang, K. Li, X. Ge, et.al, "Smart Households' Aggregated Capacity Forecasting for Load Aggregators under Incentive-based Demand Response Programs," *IEEE Trans. Ind. Appl.*, Early Access, Jan. 2020. DOI: 10.1109/TIA.2020.2966426.

[31] Jun, Z., Junfeng, L., Jie, W., Ngan, H.W., "A multi-agent solution to energy management in hybrid renewable energy generation system", *Renew. Energy*, 2011, **36**, 1, pp. 1352–1363.

[32] Kangping Li, Fei Wang, Zengqiang Mi, Mahmoud Fotuhi-Firuzabad, Neven Duić, Tieqiang Wang, "Capacity and output power estimation approach of individual behind-the-meter distributed photovoltaic system for demand response baseline estimation", *Appl. Energy*, 2019, **253**, 113595.

[33] David Wood, "Small wind turbines, Analysis, design, and application", Springer-Verlag book company, 2011.

[34] D. T. Nguyen, and L. B. Le, "Optimal Bidding Strategy for Microgrids Considering Renewable Energy and Building Thermal Dynamics", *IEEE Trans. Smart Grid*, 2014, **5**, no. 4, pp. 1608-1620.

[35] Sakawa M, Kato K, Ushiro S., "Operational planning of district heating and cooling plants through genetic algorithms for mixed linear programming", *J. Oper. Res.*, 2002, **137**, pp. 677–687.

[36] Mehdi Neyestani, Malihe M. Farsangi, Hossein Nezamabadi-pour, Kwang Y. Lee, "A modified particle swarm optimization for economic dispatch with non-smooth cost functions", *IFAC proceedings,* 2009, **42,** 9, pp. 267-272.

[37] Kangping Li, Liming Liu, Fei Wang, Tieqiang Wang, Neven Duić, Miadreza Shafie-khah, João P.S. Catalão, " Impact factors analysis on the probability characterized effects of time of use demand response tariffs using association rule mining method," *Energy Convers. Manage.* , 2019, **197**, 111891.

[38] Morteza Nazari-Heris, Mohammad Amin Mirzaei, Behnam Mohammadi-Ivatloo, Mousa Marzband, Somayeh Asadi, "Economic-environmental effect of power to gas technology in coupled electricity and gas systems with price-responsive shiftable loads", *J. Cleaner Production,* 2020, **244**, 118769.

[39] Mahdi Pourakbari-Kasmaei, Matti Lehtonen, Mahmude Fotuhi-Firuzabad, Mousa Marzband , José Roberto Sanches Mantovani, “Optimal power flow problem considering multiple-fuel options and disjoint operating zones: A solver-friendly MINLP model”, *Int. J. Electr. Power Energy Syst*., 2019, **113**, pp. 45-55.

[40] R. Ghorani, M. Fotuhi-Firuzabad, et al, "Main Challenges of Implementing Penalty Mechanisms in Transactive Electricity Markets," *IEEE Tran. Power Syst*., 2019, **34**, 5, pp.3954-3956.

[41] R. Ghorani, H. Farzin, et al, "Market design for integration of renewables into transactive energy systems," *IET Renew. Power Gener*., 2019, **13**, 14, pp 2502-2511.

[42] Z. Zhen, S. Pang, F. Wang, K. Li, Z. Li, H. Ren, et al, "Pattern classification and PSO optimal weights based sky images cloud motion speed calculation method for solar PV power forecasting," *IEEE Trans. Ind. Appl*., 2019, **55**, 4, pp.3331-3342.

[43] K. Li, Q. Mu, F. Wang, Y. Gao, et al, "A business model incorporating harmonic control as a value-added service for utility-owned electricity retailers," *IEEE Trans. Ind. Appl*., 2019, **55**, 5, pp.4441-4450.

[44] M. Song, W. Sun, Y. Wang, M. Shahidehpour, et al, "Hierarchical Scheduling of Aggregated TCL Flexibility for Transactive Energy in Power Systems," *IEEE Trans. Smart Grid*, 2019, Early Access, DOI: 10.1109/TSG.2019.2955852.

[45] A. Immanuel Selvakumar ; K. Thanushkodi, “A new particle swarm optimization solution to nonconvex economic dispatch problems”, , *IEEE Trans. On Power Systems*, 2007, **22**, 1, pp. 42-51.

[46] Ruhul Sarkar, Masoud Mohammadian, Xin Yao, “Evolutionary optimization”, Kluwer academic publishers, 2002.

[47] S. Sumathi , T. Hamsapriya , P. Surekha, “Evolutionary intelligence: An introduction to theory and applications with Matlab”, pringer-Verlag book company, 2008.

[48] El-Khattam, W. and Hegazy, Y. G. and Salama, M. M. A., “An integrated distributed generation optimization model for distributed system planning”, *IEEE Trans. On Power Systems*, 2005, **20**, pp. 1158-1165.

[49] Farid Varasteh, Mehrdad Setayesh Nazar, Alireza Heidari, Miadreza Shafie-khah, João P. S. Catalão, “Distributed energy resource and network expansion planning of a CCHP based active microgrid considering demand response programs”, *Energy*, 2019, **172**, pp. 19-105.

[50] Mohsen Kia, Mehrdad Setayesh Nazar, Mohammad Sadegh Sepasian, Alireza Heidari, and João P. S. Catalão, “New framework for optimal scheduling of combined heat and power with electric and thermal storage systems considering industrial customers inter-zonal power exchanges”, *Energy*, 2017, **138**, (1), pp. 1006-1015.

[51] Available at: http://www.ece.ufrgs.br/~gmasp/m123b.html